

70551

ROUGHNESS OF SAND BEDS : DEVELOPMENT OF MODELS

A Thesis Submitted
In Partial Fulfilment of the requirements
for the Degree of
MASTER OF TECHNOLOGY

by
SHEO PRASAD SINGH

to the
DEPARTMENT OF CIVIL ENGINEERING
INDIAN INSTITUTE OF TECHNOLOGY KANPUR
DECEMBER, 1981

117 07 APR

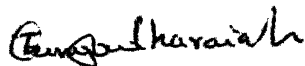
1000 07 APR

Ann. No. 70554

20 APR 1982

CERTIFICATE

This is to certify that the thesis 'ROUGHNESS OF SAND BEDS: DEVELOPMENT OF MODELS' submitted by Shri S.P. Singh, in partial fulfilment of the requirements for the Degree of Master of Technology at the Indian Institute of Technology, Kanpur has been carried out under my supervision and guidance. The work embodied in this thesis has not been submitted elsewhere for award of a degree.



December, 1981

(Dr. T. Gangadharaiah)
Assistant Professor
Department of Civil Engineering
Indian Institute of Technology, Kanpur

ACKNOWLEDGEMENTS

The author wishes to express his sincerest gratitude and appreciation to his thesis advisor Dr. T. Gangadharaiah for his valuable guidance, inspiration and encouragement during the course of this research.

The author expresses his sincere thanks to:

- Staff of the Hydraulics and Water Resources Engineering.
- Dr. V.K. Garg for providing the wind tunnel facilities of his laboratory.
- Mr. B.S. Rohewal and Mr. Suresh Kumar for his valuable helps in the experimental programme.
- Staff of the Hydraulics and Water Resources Laboratory for their timely helps.
- Dr. K.J. David , M/s Alok Sarin, R.L. Sharma, K.V. Jay Kumar, A.K. Mishra, K.K. Agarwal, Vinay Kumar, R. Kumar, D.P. Singh, S.S. Singh, Miss Bibha Das, my friends, for their selfless service rendered at various stages during my stay at I.I.T. Kanpur.
- And finally thanks to Mr. S.N. Pandey and Mr. G.S. Trivedi for their excellent typing work.

S.P. SINGH

ABSTRACT

Resistance to flow on a rigid flat beds having randomly spaced uniform sand grains and densely packed nonuniform sand grains was investigated, to cover the transitional state of flow. The median size of the sand grains used was of 1.5 mm. The roughness of sand beds are represented in terms of Nikuradse's equivalent sand grain roughness K_s/d_{50} and shift in velocity scale $\Delta u^+ = 1/\kappa \ln d_{50}^+$. Based on the present experimental results and results of previous investigations carried out at this Institute, models to represent the roughness of sand beds in terms of geometry of the beds represented by roughness concentration and nonuniformity parameter σ/d_{50} and flow parameter represented by Grain Shear Reynolds number $\frac{V_* d_{50}}{\nu}$ has been developed. These models predict the roughness of sand beds fairly well.

CONTENTS

CHAPTER		Page
	CERTIFICATE	i
	ACKNOWLEDGEMENTS	ii
	ABSTRACT	iii
	CONTENTS	iv
	FIGURES	vii
	NOTATIONS	viii
I	INTRODUCTION AND LITERATURE REVIEW	1
	A Introduction	1
	B Relevant Literature Review	2
	C Shift in Velocity and Length Scale	6
	D Theoretical Bed Level	8
	E Present Investigation	9
II	METHODOLOGY	11
	A Details of Wind Tunnel	11
	B Preparation of Rough Beds	12
	C Measurement of Velocity Profiles	14
	D Measurement of the Grain Surface Profiles of the Sand Beds	19
	E Compilation of Data	21
	(a) Mean velocity data	21
	(b) Deduction of parameters	21

III	ANALYSIS AND DEVELOPMENT OF MODELS	24
A	General	24
B	Mean Velocity Distribution	24
	(a) Law of Wall	26
	(b) Velocity Defect Law	31
C	Functional Relationships for Roughness of Sand Grain Beds	31
	(a) Effect of concentration on roughness of uniform sand grains randomly distributed	34
	(i) Nikuradse's equivalent sand grain roughness (K_s)	34
	(ii) Shift in velocity scale $\Delta u/V_*$	36
	(iii) Theoretical bed level	38
	(b) Effect of nonuniformity in grain size on roughness of sand beds densely covered by the grains	40
	(i) Nikuradse's roughness function(K_s)	40
	(ii) Shift in velocity scale Δu^+	42
	(iii) Theoretical bed level	46
D	Model for Roughness Scale	46
	(a) Model based on the geometry of the rough bed profiles	48
	(b) Model for roughness of uniform grains randomly spaced	54
	(c) Model for roughness of sand beds having nonuniform sand grains densely packed	56
	(i) Functional relationship between theoretical bed level and $d_{50}V_*/\gamma$ and σ/d_{50}	58

	(ii) Functional relationship among Δu^+ , e^+ , d_{50}^+ and c^*/d_{50}	59
	(iii) Model for roughness scale	63
E	General Comments	66
IV	CONCLUSIONS AND RECOMMENDATIONS	68
A	General	68
B	Conclusions	69
C	Recommendations	69
V	BIBLIOGRAPHY	71
VI	APPENDIX	74

FIGURES

Figure		Page
1	General layout of wind tunnel	13
2	Grain size distribution for 1.5 D sand bed Series	15
3	Grain size distribution for 1.5 DS sand bed series	16
4	Law of the wall for 1.5 DS sand bed series	27
5	Law of the wall for 1.5 D sand bed series	28
6	Law of the wall using roughness scale for 1.5 DS sand bed series	29
7	Law of the wall using roughness scale for 1.5 D sand bed series	30
8	Velocity defect law for 1.5 DS sand bed series	32
9	Velocity defect law for 1.5 D sand bed series	33
10	Effect of roughness concentration on K_s	35
11	Effect of roughness concentration on the law of the wall intercept	37
12	Effect of roughness concentration on the theoretical bed level	39
13	Effect of nonuniformity in grain size on effective roughness scale K_s	41
14	Variation of Δu^+ with d_{50}^+ for selected values of σ/d_{50}	43
15	Effect of nonuniformity on the law of wall	45
16	Effect of nonuniformity on the theoretical bed level	47
17	Autocorrelation and spectral density of 1.5 D and 1.5 DS sand bed series	49
18, 19, 20	Variation of H_s/d_{50} with σ/d_{50} , $\Delta u^+ - \frac{1}{\chi} \ln e^+$ with χ , $\sigma^+ d_{50}^+$ with e/d_{50}	53, 60 61
21	Variation of $\Delta u^+ - \frac{1}{\chi} \ln e^+$ with $\sqrt{\sigma^+ d_{50}^+}$	62

NOTATIONS

B, B_s, B_R, B_*, C_1	Constants
d	Diameter of the sand grain
d_{50}	Grain size through which 50 percent of sample is passed
d_{65}	Grain size through which 65 percent of sample is passed
d_{85}	Grain size through which 85 percent of sample is passed
d_{90}	Grain size through which 90 percent of sample is passed
\bar{h}	Mean height of roughness grains
K_s	Nikuradse's equivalent sand grain roughness factor
\bar{u}	Time average velocity of air at any height y
U_∞	Free stream velocity of air in the test section
V_*	Shear velocity, $V_* = \left(\frac{\tau_0}{\rho}\right)^{1/2}$
$\frac{\Delta \bar{u}}{V_*}$	Shift in velocity scale
$\frac{V_* d_{50}}{\nu}$	Grain Shear Reynolds number based on d_{50} ($Re_* = \frac{V_* d_{50}}{\nu}$)
y_t	Perpendicular height from the theoretical bed level ($y_t = y - \delta$)
y	Distance (Ordinate) measured perpendicular to the bed from the top of the grain.
S_0	Zeroth moment of spectral function
S_2	Second moment of spectral function
S_4	Fourth moment of spectral function
m	Spectral parameter
H_s	Significant height ($H_s = 4 h^m$)

\bar{a}	Average amplitude of sand grain beds
σ_a	Standard deviation of amplitudes
\bar{s}	Average spacing
σ_s	Standard deviation of spacings

Greek alphabets

δ	Boundary layer thickness measured from the top of grain
δ_t	Boundary layer thickness measured from the theoretical bed level ($\delta_t = \delta - \epsilon$)
ϵ	The location of the apparent origin for velocity distribution above the smooth surface of the flat bed
χ	Von Karman's universal constant
ρ_a	Mass density of air
σ	Standard deviation for the diameter (size) of sand grains
ν	Kinematic viscosity (air)
λ	Roughness concentration
γ_f	Specific weight of fluid (air)
γ_s	Specific weight of solid (sand grains)

CHAPTER I

INTRODUCTION AND LITERATURE REVIEW

A. Introduction

The flow phenomena in rivers, canals and deserts are controlled by roughness of sand beds. Before initiation of motion of sand grains, roughness of sand beds can be considered similar to flow over rigid beds. Nikuradse, as early as 1933, developed methodology for rough wall flow analysis by investigating flow in pipes having their walls roughened with uniform sand grains glued closely. Schlichting developed roughness scale for other roughness which are less densely placed and called it as equivalent sand grain roughness and is denoted as K_s . There was no systematic investigation on the roughness of sand beds till recently. Investigations carried out by P.K. Mittal and S. Mittal showed the importance of nonuniformity of sand grains in sand beds, for completely rough turbulent flows. David investigated the roughness of sand beds for transitional and smooth turbulent flows. It was found that roughness, denoted in terms of Nikuradse's equivalent sand grain roughness varies with state of flow and nonuniformity in sand grain size distribution. There was wide gap in the transition region to fully rough turbulent regions in the

above experimental series. Here an attempt to investigate this region has been made.

Roughness of sand beds can be predicted by using correlations curves developed by David. An attempt to develop model for rough turbulent flow on sand bed was made by David. This model can not be extended for transitional state of flow. Development of model to predict roughness of sand beds for rough turbulent and transitional regions was of necessity. Here an attempt to develop model for roughness scales in terms of geometry of bed surface and flow properties has been attempted.

B. Relevant Literature Review

Nikuradse developed a frame work of rough wall flow analysis by investigating flow in sand roughened pipes. Nikuradse's investigations showed that the effect of roughness on the velocity profile was confined to a thin layer near the wall. The velocity distribution in this layer follows a logarithmic function. This is universal in character and is determined only from the wall conditions and distance from the wall. According to the current view, the velocity distribution in the logarithmic zone does not differ whether it is boundary layer flow, pipe flow or free surface flow (Monin and Yaglom, 1971; Hinze, 1975).

After Nikuradse's investigations, the work of Schlichting's (1936) experiments revealed that, for rough surfaces having lesser concentration of elements, the roughness parameter was different from the size of the roughness element. Schlichting showed that the roughness effect is a function of the average height of the roughness elements and also of their size, shape and concentration distribution over the wall surface. Therefore, in order to characterise roughness, he made use of 'Nikuradse's equivalent sand grain roughness, K_s ', which is defined as the size of the uniform sand grain that, produces the same resistance coefficient as the actual roughness under the same flow condition. Using K_s , to represent both uniform and nonuniform roughness, the velocity distribution in the logarithmic zone is written as

$$\frac{u}{v_*} = \frac{1}{\kappa} \ln (y/K_s) + B (v_* K_s/\nu) \quad (1)$$

Based on the concept of Nikuradse, to represent K_s in terms of particular size of sand grains, is usual practice in sediment transport studies. To name a few of the studies:

Einstein and Barbarossa (1952) considered $K_s = d_{65}$
 Simons and Richardson (1966) utilized $K_s = d_{85}$ whereas
 Kamphuis (1974) used $K_s = 2d_{90}$.

Colbrook and White (1937) investigated how resistance would be affected by adding a small but definite proportion of large grains to uniform fine grains. They observed that the presence of larger grains, though only in small proportion, considerably affects the resistance mechanism due to their shielding effect on finer grains and thus reduces the effectiveness of smaller grains. Their results also indicate that roughness concentration is not a good parameter to deal with nonuniform roughness, while it is useful for uniform roughness. This is because 'concentration' becomes vague when the whole area of bed is covered by sand grains.

O'Loughlin and MacDonald (1964) did experiments on sand grains as roughness elements randomly spaced in the various concentrations. According to them, the difference in resistance offered by regularly arranged spheres and irregularly arranged sand grains is due to the irregularity in shape and the randomness in arrangement.

It may be noted that representation of K_s in terms of any particular size is not proper, instead parameters describing the distribution of sand grains namely median size d_{50} and standard deviation σ may be better parameters. P.K. Mittal and S. Mittal conducted experiments to find the effect of nonuniformity in

grain size represented in terms of σ/d_{50} on the roughness scale K_s . They observed that for coarse sand grains, K_s/d_{50} is a unique function of nonuniformity coefficient σ/d_{50} and is independent of Grain Shear Reynolds number, $\frac{d_{50} V_*}{\nu}$. David conducted a through investigation to find the effect of Grain Shear Reynolds number $\frac{d_{50} V_*}{\nu}$ along σ/d_{50} on K_s/d_{50} . David showed from his experiment for $V_* d_{50}/\nu = 60, 24$ and 8 that the functional form K_s/d_{50} with σ/d_{50} do not coincide with higher $\frac{V_* d_{50}}{\nu}$ value, but follow different curves for each range.

It may be observed that the gap in d_{50}^+ values between P.K. Mittal and Sudhir Mittal data and David's data was wide, so a necessity was felt to investigate for d_{50}^+ values that lies between 200 and 60. Also there is a necessity to develop an analytical relationship between K_s/d_{50} and σ/d_{50} for various d_{50}^+ . Here an attempt is made to investigate experimentally the effect of nonuniformity in grain size on roughness scale for d_{50}^+ order of 100. Based on experimental data, a method to predict K_s/d_{50} by knowing σ/d_{50} and d_{50}^+ is also attempted.

Investigations of Schlichting (1936), O'Loughlin and MacDonald (1979), David (1980) and Sarin (1980) showed that the arrangement pattern, shape and relative

size of the roughness element are important. The roughness concentration defined as the ratio of the projected area of the grains to the total area of the bed is used to represent one of the geometrical parameters of uniform roughness elements when sparsely distributed on the bed. In the case of densely packed sand grain beds, the nonuniformity parameter σ/d_{50} is considered to represent the geometry scale of the sand bed.

G. Shift in Velocity and Length Scales

Another form of representing roughness, is in terms of shift in velocity scale and shift in length scale.

This method was introduced by Hama (1954). Here, the roughness effect is considered equivalent to shift in the velocity profile from smooth wall to rough wall by a value $\Delta u/V_* = u^+$ and is written as

$$\left(\frac{u}{V_*}\right)_{\text{rough}} = \left(\frac{u}{V_*}\right)_{\text{smooth}} - \frac{\Delta u}{V_*} \quad (2)$$

where

$$\left(\frac{u}{V_*}\right)_{\text{smooth}} = \frac{1}{\alpha} \ln y^+ + B_s$$

and

$$\left(\frac{u}{V_*}\right)_{\text{rough}} = \frac{1}{\alpha} \ln y/K_s + B_R$$

in which $y^+ = \frac{y V_*}{\nu}$; B_s and B_R are constants for smooth

and completely rough beds. Using these expressions, the shift in velocity u^+ may be represented in terms of z_S and z_R as

$$\Delta u^+ = \frac{1}{\kappa} \ln K_s^+ + (z_S - z_R) \quad (4)$$

Hama related K_s with u^+ as

$$\Delta u^+ = 5.6 \log (K_s^+ + 3.3) - 2.92$$

For fully rough turbulent flow condition, Hama (1954) and Clauser (1956) determined the value of u^+ for different types of roughness. Batterman showed that $u^+ - \frac{1}{\kappa} \ln K^+$; is a function of roughness concentration for two-dimensional roughnesses.

Perry et al. (1969) investigated the following relation

$$\Delta u^+ = \frac{1}{\kappa} \ln \frac{V_* \epsilon}{\nu} + C_1 \quad (6)$$

The value of ϵ was found to be varying with geometry of the roughness scale and also with state of flow (d_{50}^+).

P.K. Mittal, S. Mittal and David showed that the function $u^+ - \frac{1}{\kappa} \ln K^+$ is a function of ϵ/d_{50} and d_{50}^+ for nonuniform sand grains densely packed. David, Sarin and Aslam showed that the function $u^+ - \frac{1}{\kappa} \ln d_{50}^+$ is a function of roughness concentration and d_{50}^+ for

uniform grains randomly spaced (acting as 3-dimensional roughnesses).

D. Theoretical Bed Level : z

The velocity distribution on a rough wall behaves as if its origin is located at some distance, z_t below the crest of the roughness elements (Moore, 1951).

Blanco and Partheniades (1971) found a relation for uniform densely packed bed

$$z_t = 0.27 K_s \quad (7)$$

Einstein and El-Samni (1949) had also obtained this relation for pebbles. Kamphuis (1974) assumed that the virtual bottom is $0.7 d_{50}$ above the plane to which the sand grains were attached. David showed that the z/d_{50} is a function of G/d_{50} and d_{50}^+ (where 'z' is a distance measured from plane surface to the theoretical bed level). For d_{50}^+ values greater than 220, the value of z/d_{50} was less than unity. For $d_{50}^+ < 220$, it was observed that the theoretical bed level was much above d_{50} level. David, Sarin and Aslam showed that the theoretical bed level coincides with the geometric bed level for uniform sand grains and glass beads sparsely distributed for rough turbulent flow conditions.

E. Present Investigation

An investigation on the roughness characteristics of sand grain beds was planned as a continuing study. The nonuniformity parameter defined as σ/d_{50} was varied to study the roughness characteristics with nonuniformity of sand grains.

Under this programme, P.K. Mittal (1977) carried out experiments on rough surfaces represented by sand grain beds having a median diameter (d_{50}) of 1 mm, 2 mm, 4 mm, 6 mm and 8 mm. The nonuniformity of bed was obtained by varying the standard deviation of sizes to 2-3 values.

S. Mittal (1978) worked on one median size ($d_{50} = 3.0$ mm) but varied σ to about 10 different values. David (1980) investigated 3 series of sand beds having $d_{50} = 0.14$ mm, 0.39 mm and 0.925 mm. Each series had a number of beds with different σ/d_{50} . Sarin investigated the effect of roughness concentration of size 0.925 mm sand grains and 3.0 mm glass beads on the roughness scales K_s/d_{50} , $\Delta u^+ - \frac{1}{\alpha} \ln d_{50}^+$ and ϵ/d_{50} .

The present work is planned to investigate the following aspects:

- (1) The effect of nonuniformity in sand grains size with median value 1.50 mm to relate the work of P.K. Mittal, S. Mittal and David.

- (2) Experiments of uniform size with $d_{50} = 1.5 \text{ mm}$ for different roughness concentrations were planned to find the effect of randomness in spacing on roughness scales.
- (3) To develop a geometrical parameter to represent the roughness scales for above cases.
- (4) To develop a method to predict K_s/d_{50} by knowing σ/d_{50} and d_{50}^+ .

CHAPTER II

METHODOLOGY

A. Details of Wind Tunnel

An open circuit wind tunnel with closed test tube section is used. A honeycomb is located at one end of the wind tunnel along with five screens of size 1.25 m x 1.25 m through which air enters into the test section. The honeycomb-cum-screen portion is 2.3 m long, after which there is a contraction which leads to the test section. The test section is 0.4 m square and 4 m long. From the test section there is a gradual expansion which leads to a circular section of diameter 1.0 m. At this end is fitted an exhaust fan of 1.0 m dia which sucks air through the test section. The exhaust fan is operated by a motor of 3.7 kw, 5 hp and 960 rpm.

For controlling the velocity of air in the test section, there is a pair of adjacent gates fitted at the end of the test section. When the gates are completely closed the maximum possible velocity is obtained. The gates can be operated and kept at a desired opening to get four different velocities approximately 19.0 m/sec., 17.0 m/sec., 14.0 m/sec and 11.0 m/sec.

Five stations in the test section at distances of 0.14 m, 1.04 m, 1.94 m, 2.84 m and 3.73 m from the leading edge of the test section were chosen at which measurement of velocity was taken. A small hole is provided on the side of the test section at each of these sections for static pressure measurements. A total head tube, having 9 mm outside diameter and 5.0 cm long is used for the measurement of total head pressure. This total head tube is attached to a traversing mechanism which can move in the vertical direction with 0.05 mm least count. The total head tube and the static pressure tap hole on the side of the test section are connected to a differential manometer which can read to an accuracy of 0.00254 cm of water. A layout of the wind tunnel is shown in Fig. 1.

B. Preparation of the Rough Beds

A set of two plane and smooth wooden boards, completely occupying the test section floor of the wind tunnel, were used to prepare one rough bed. A thin coat of paint was evenly applied over one side of the board. Roughness elements of known weight were sprinkled over this surface to get a random arrangement. The bed was allowed to dry, without disturbance, for about 40 hrs. When the paint dried completely, the bed was upturned

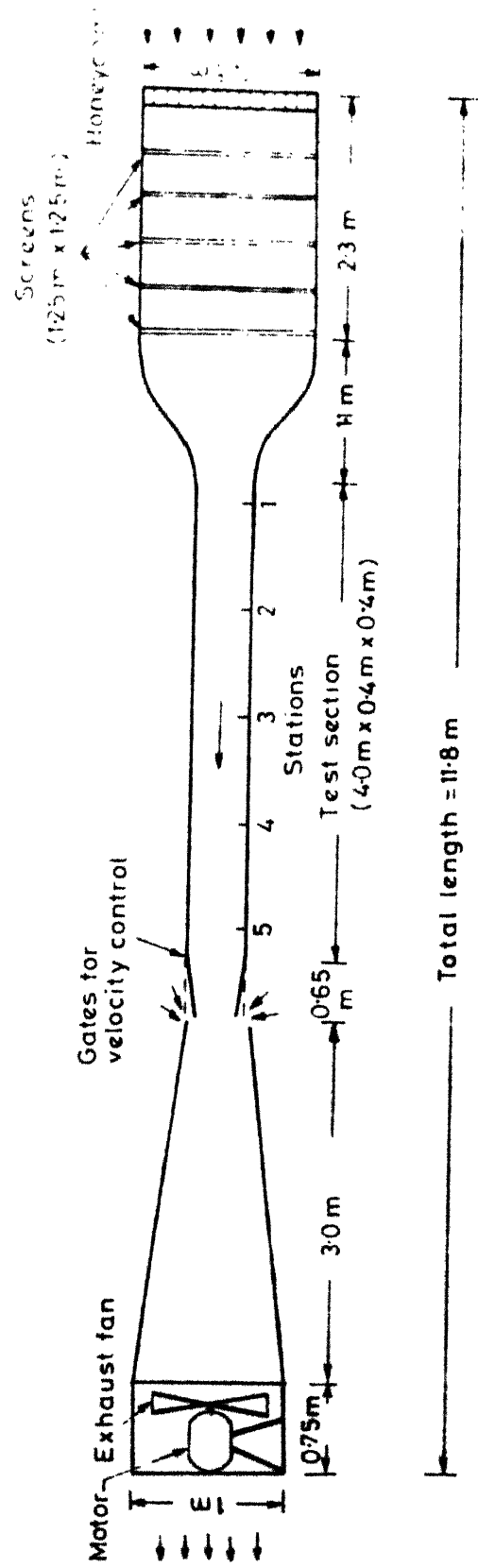


FIG. 1.1 LAYOUT OF WIND TUNNEL

se that the unstruck elements fall out. The total weight of the sticking elements were analysed and distribution curves are given in Fig. 2 and Plate 1. Using these curves, the value of nonuniformity coefficient σ/d_{50} was calculated. For beds having uniform grains randomly spaced, the spacing was measured. The distribution of spacing values for each bed is shown in Fig. 3 and Plate 2.

C. Measurement of Velocity Profiles

The wooden boards constituting the rough beds were laid on the test section of the wind tunnel and were fixed to the floor of the test section by a set of bolts which were flush with the painted surface of the bed. The leading edge of the bed had a smooth taper in order to join with the floor of the tunnel.

The desired free stream velocity through the test section was obtained by adjusting the gates to a particular opening. Four different free stream velocities were used for each bed, which were approximately 19.0 m/sec., 17.0 m/sec., 14.0 m/sec and 11.0 m/sec. For each of these free stream velocities a minimum of one velocity profile was taken along the centre line of the bed at each of the five stations. On the average, the number of velocity profiles taken on each bed ranged between 16 to 20.

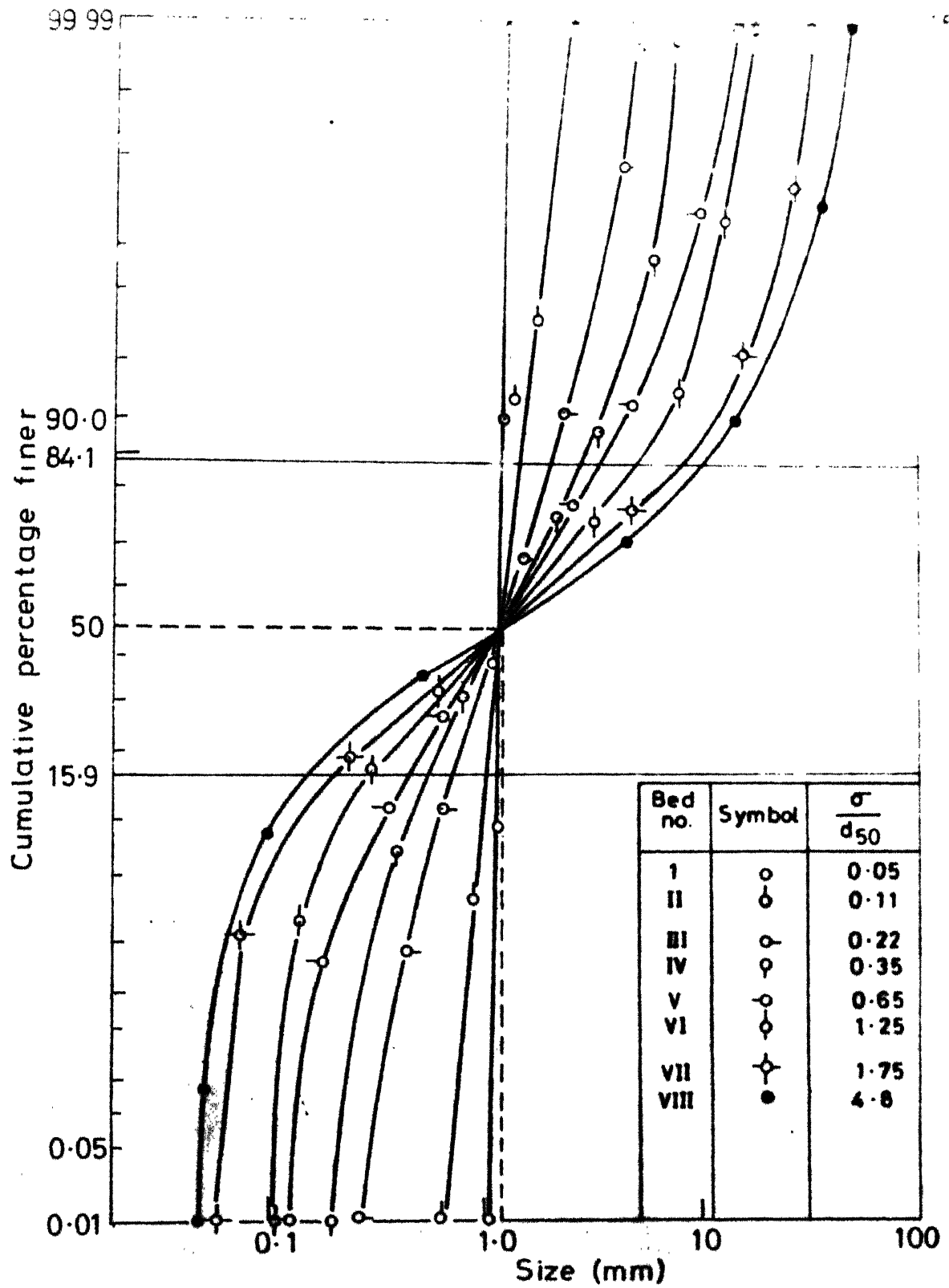


FIG. 2 GRAIN SIZE DISTRIBUTION FOR 1.5 D SERIES BEDS

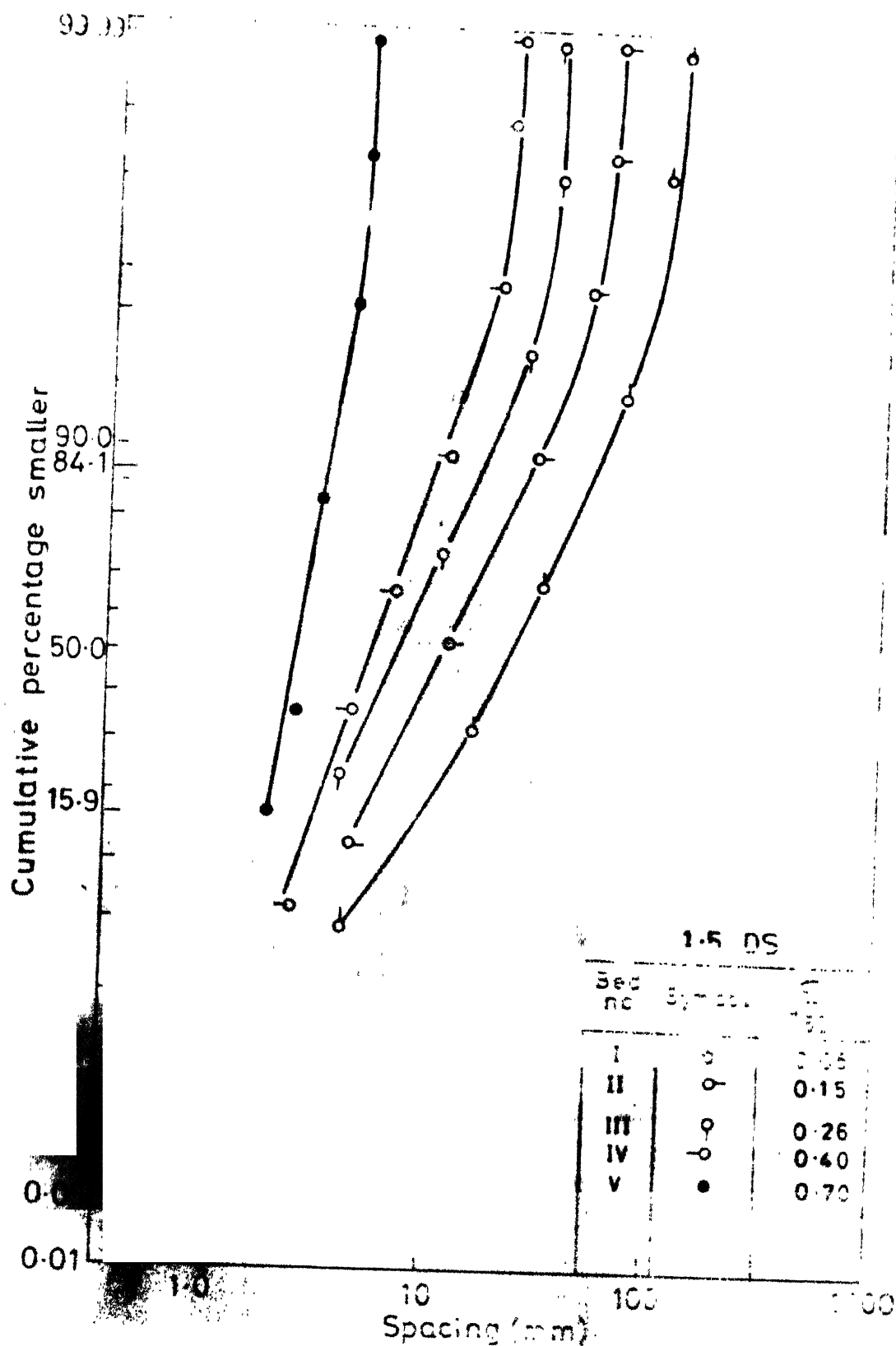


FIG. 3 SPACING DISTRIBUTION FOR 1.5 DS SEALED SMALL AREA

For velocity measurement, two manometers (depending upon the range of pressure) and a total head tube (or probe) with a vernier scale and slow moving device was used. The static pressure end of the manometer was connected to the static tap hole on the side of the test section and the other end was connected to the total head tube. The room temperature was noted for each test.

Once the required free stream velocity was maintained in the test section, the probe was lowered down to the bed at each station. Near to the bed, the pressure measurements were taken at very close intervals (0.5 mm or less), and at increasing distances from the bed. The interval was gradually increased to 1 mm, 2 mm, 3 mm, 5 mm etc. since that part of the boundary layer covering the wall region is very important in data reduction, care was taken to get a minimum of 10 readings in the region extending from 5 percent to 15 percent of the boundary layer thickness.

D. Measurement of the Grain Surface Profiles of the Sand Beds

Two specimens of each bed of 1.5.D sand bed series had been prepared on glass plates for grain surface measurements. The glass plates were of size 8 cm x 20 cm and were given a thin coat of paint and laid side by side with the painted wooden boards used in the preparation of the beds. The sand was sprinkled over the glass plates and the

boards at the same time and in the same manner that there was no difference between the glass plate portion and wooden board portion of the bed except that the wooden board portion was tested in the wind tunnel while the glass plate portion was used for grain surface measurements.

A sand surface profile meter developed by David was used in the profile measurements. It essentially consisted of a needle point which could move both in horizontal and vertical directions by means of horizontal and vertical transverse mechanism. In both directions verniers could be read, the least count of the vertical vernier was 0.05 mm and that of the horizontal one was 0.1 mm. The glass plate model of the bed was placed underneath the needle point. The horizontal alignment of the glass plates and the base of the apparatus could be checked by a spirit level.

The initial readings were taken by lowering the needle to touch the smooth portions of the glass plates. Now the needle was raised up, traversed along the centre line of the bed, lowered to touch the grain surface at every 2 mm horizontal interval and the vertical vernier was read. The bottom level of the grains being known, the height of the grains could be calculated.

boards at the same time and in the same manner that there was no difference between the glass plate portion and wooden board portion of the bed except that the wooden board portion was tested in the wind tunnel while the glass plate portion was used for grain surface measurements.

A sand surface profile meter developed by David was used in the profile measurements. It essentially consisted of a needle point which could move both in horizontal and vertical directions by means of horizontal and vertical transverse mechanism. In both directions verniers could be read, the least count of the vertical vernier was 0.05 mm and that of the horizontal one was 0.1 mm. The glass plate model of the bed was placed underneath the needle point. The horizontal alignment of the glass plates and the base of the apparatus could be checked by a spirit level.

The initial readings were taken by lowering the needle to touch the smooth portions of the glass plates. Now the needle was raised up, traversed along the centre line of the bed, lowered to touch the grain surface at every 2 mm horizontal interval and the vertical vernier was read. The bottom level of the grains being known, the height of the grains could be calculated.

E. Compilation of Data

a. Mean velocity data

Velocity was measured on rough beds along the centre line of the test section at five stations, for four velocities having a magnitude equal to 11, 14, 17 and 19 m/sec. approximately. The dynamic head in the differential manometer was measured as head of water in inches. It has been converted into mean velocity \bar{u} , in m/sec. The velocity profiles were used in deduction of wall law parameters i.e. V_* , $\Delta\bar{u}/V_*$ and e .

b. Deduction of wall law parameters

Boundary layer has been divided into two regions:

- (1) Wall law region, and
- (2) Defect law region

The wall law region has been defined between $y_t/\delta_t=0.0$ to 0.2 and rest region has been defined as defect law region. The wall law region from $y_t/\delta_t = 0.05$ to 0.2 is represented by logarithmic velocity distribution.

According to Hama (1954), the wall law relationship in logarithmic region has been written as

$$\frac{u}{V_*} = \frac{1}{\kappa} \ln \frac{V_* (y - e)}{\nu} + 4.9 - \Delta u/V_* \quad (8)$$

In the above equation u and y are measured quantities and the value of λ is taken as 0.41, according to Hama. The shear velocity V_* , shift in velocity scale Δu and shift in length scale C are unknown quantities. To evaluate these three unknown quantities, least square method assisted by Newton-Raphson procedure was used. From computed values of $\Delta u/V_*$, the values of K_s/d_{50} were computed using equation

$$\Delta u^+ - \frac{1}{\lambda} \ln d_{50}^+ = \frac{1}{\lambda} \ln \left(\frac{K_s}{d_{50}} + \frac{3.3}{d_{50}^+} \right) - 3.215 \quad (9)$$

The computed data is given in Table 1 and other details of mean of heights, standard deviation of heights and spectrum moments are given in Appendix.

TABLE 1 : EXPERIMENTAL RESULTS

S.No.	$\frac{\sigma}{d_{50}}$	$\frac{v_* d_{50}}{\gamma}$	$\frac{K_s}{d_{50}}$	$\Delta u^+ - \frac{1}{\kappa} \ln d_{50}^+$	$\frac{e}{d_{50}}$	$\frac{\sigma K_s}{d_{50}}$
1	0.05	77.85	1.65	-1.5	1.730	0.159
2	0.10	103.96	2.45	-0.5	1.400	0.170
3	0.20	112.05	3.40	0.3	0.960	0.090
4	0.35	133.52	4.20	0.7	0.915	0.120
5	0.65	133.62	4.65	1.0	0.905	0.200
6	1.25	86.10	4.25	0.7	0.900	0.080
7	1.75	77.82	3.70	0.2	0.750	0.110
8	4.80	72.00	2.05	-1.3	0.452	0.140

S.No.	λ	$\frac{V_* d_{50}}{\gamma}$	$\frac{K_s}{d_{50}}$	$\Delta u^+ - \frac{1}{\kappa} \ln d_{50}^+$	$\frac{e}{d_{50}}$	$\frac{\sigma K_s}{d_{50}}$
1	0.05	110.84	1.05	-2.90	0.690	0.060
2	0.15	110.26	2.00	-1.02	0.850	0.100
3	0.26	134.17	2.40	-0.67	1.060	0.090
4	0.40	107.09	2.33	-0.74	1.010	0.150
5	0.70	90.35	1.72	-1.40	1.730	0.120

CHAPTER III

ANALYSIS AND DEVELOPMENT OF MODELS

A. General

This chapter is devoted to the analysis of results deduced for turbulent flows over all roughness beds tested in the present investigation. Whenever required, the results stated by Schlichting (1936), O'Loughlin et al. (1964), David (1980), P.K. Mittal (1977), S. Mittal (1978), Srin (1980) and Aslam (1981) are reproduced. Using these data, roughness parameters have been studied. Models for roughness parameters (K_s/d_{50}) and $\Delta u^+ = \frac{1}{\kappa} \ln d_{50}^+$ in terms of σ/d_{50} or λ and $d_{50} \frac{V^*}{\nu}$ have been developed.

B. Mean Velocity Distributions

Mean velocity profiles in a boundary layer flow can be represented as

$$\frac{\bar{u}}{V^*} = f\left(\frac{V^* y}{\nu}, \frac{y}{\delta}\right) \quad (10)$$

The velocity distribution near the wall is

$$\frac{\bar{u}}{V_*} = f(V_* y/\nu) \quad (11)$$

The velocity distribution in the **outer** zone is

$$\frac{\bar{u}}{V_*} = f(y/\delta) \quad (12)$$

These functional representations have been described as follows:

(i) Prandtl's wall law

$$\frac{\bar{u}}{V_*} = \frac{1}{\kappa} \ln \frac{V_* y}{\nu} + B \quad (B = 4.9 \text{ for smooth bed}) \quad (13)$$

according to Hanna

(ii) Karman's velocity defect law

$$\frac{U_\infty - \bar{u}}{V_*} = \frac{1}{\kappa} \ln y/\delta + B_* \quad (14)$$

($B_* = 2.9$ for smooth bed according to Hinze).

Whereas B and B_* are functions of flow and geometry of roughness.

Mean velocity profiles obtained from all roughness beds under the present investigation can be represented in two ways. Velocity profiles have been presented only for station 5 and for velocity of magnitude 19.0 m/s only.

2. Law of wall

(i) $\frac{\bar{u}}{v_*}$ as a function of $\frac{v_* y_t}{\nu}$

Velocity profiles in terms of $\frac{\bar{u}}{v_*}$ have been plotted against $\frac{v_* y_t}{\nu}$ where $y_t = y - z$ for all the beds in Figs. 4 and 5. Here velocity distribution for each bed follows a straight line parallel to one another.

The velocity profile for roughness bed in the region of $\lambda = .25$ or $\delta/d_{50} = .65$ has the highest value of $\Delta\bar{u}/v_*$. For variation of λ and δ/d_{50} on either side of these values, respectively, $\frac{\Delta\bar{u}}{v_*}$ decreases systematically. The velocity profiles indicate that $\frac{\Delta\bar{u}}{v_*}$ is function of surface characteristics λ or δ/d_{50} of the bed.

(ii) $\frac{\bar{u}}{v_*}$ as a function of y_t/K_s

The plots of $\frac{\Delta\bar{u}}{v_*}$ against y_t/K_s have been plotted in Fig. 6 and 7. These profiles fall on a single curve. There is a scatter near the wall, which is the effect of viscosity and nonuniformity in grain size. The roughness scales $\Delta\bar{u}/v_*$, $\frac{\delta}{d_{50}}$ and K_s/d_{50} are functions of roughness geometry like $\delta/d_{50}, \lambda$, and grain shear Reynolds number $\frac{d_{50} v_*}{\nu}$. The analysis of these functional

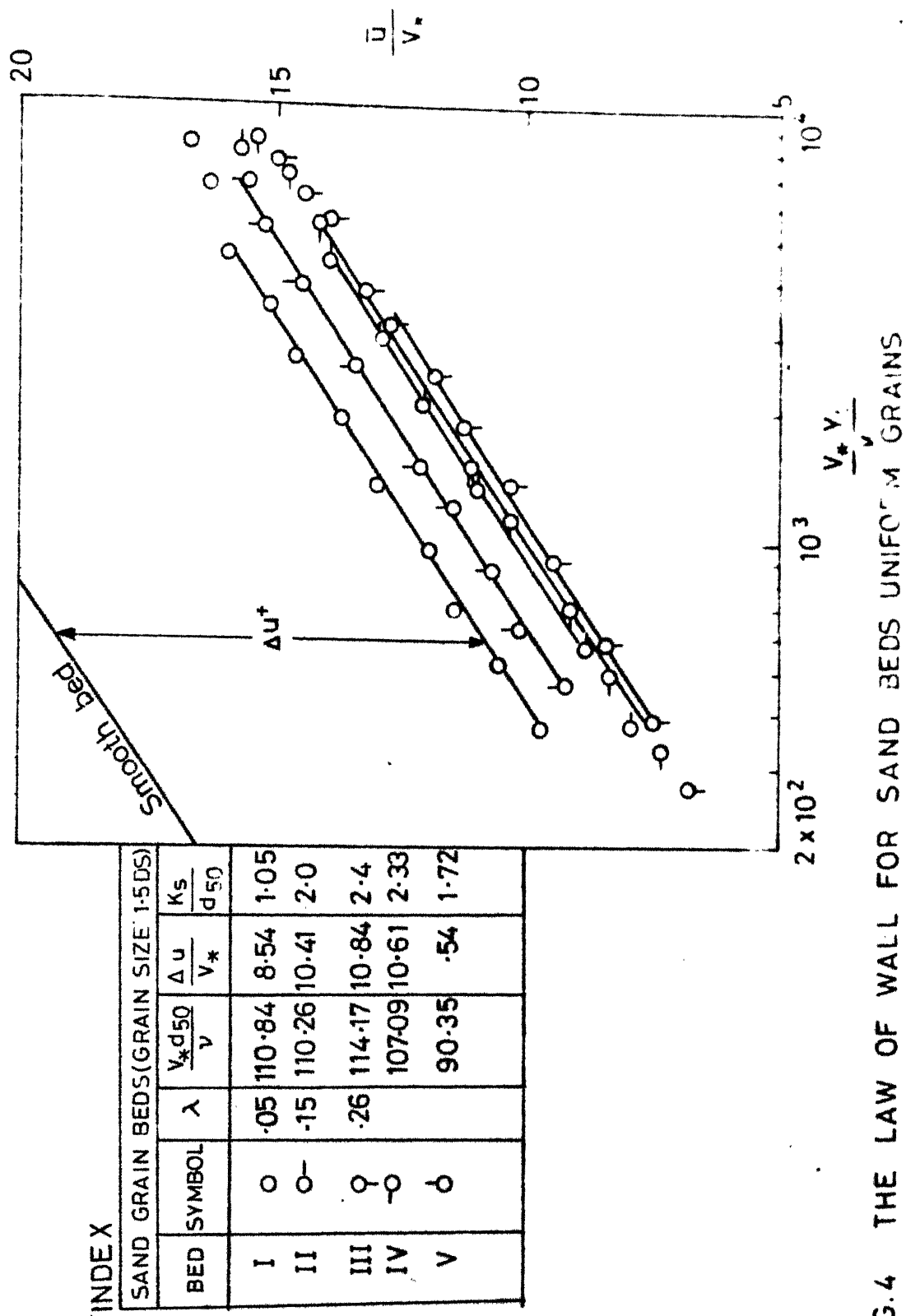


FIG.4 THE LAW OF WALL FOR SAND BEDS UNIFORM GRAINS

INDEX

1.5 D

Symbol	$\frac{\sigma}{d_{50}}$	$\frac{V_* d_{50}}{v}$	$\frac{\Delta u}{V_*}$	$\frac{K_g}{d_{50}}$
○	0.05	77.85	9.0	1.65
○-	0.10	103.96	9.5	2.45
○	0.20	112.05	10.0	3.40
○-	0.35	133.52	11.0	4.20
○	0.65	133.62	12.0	4.65
○	1.25	86.1	11.70	4.25
○-	1.75	76.82	11.5	3.70
●	4.8	72.0	11.2	2.05

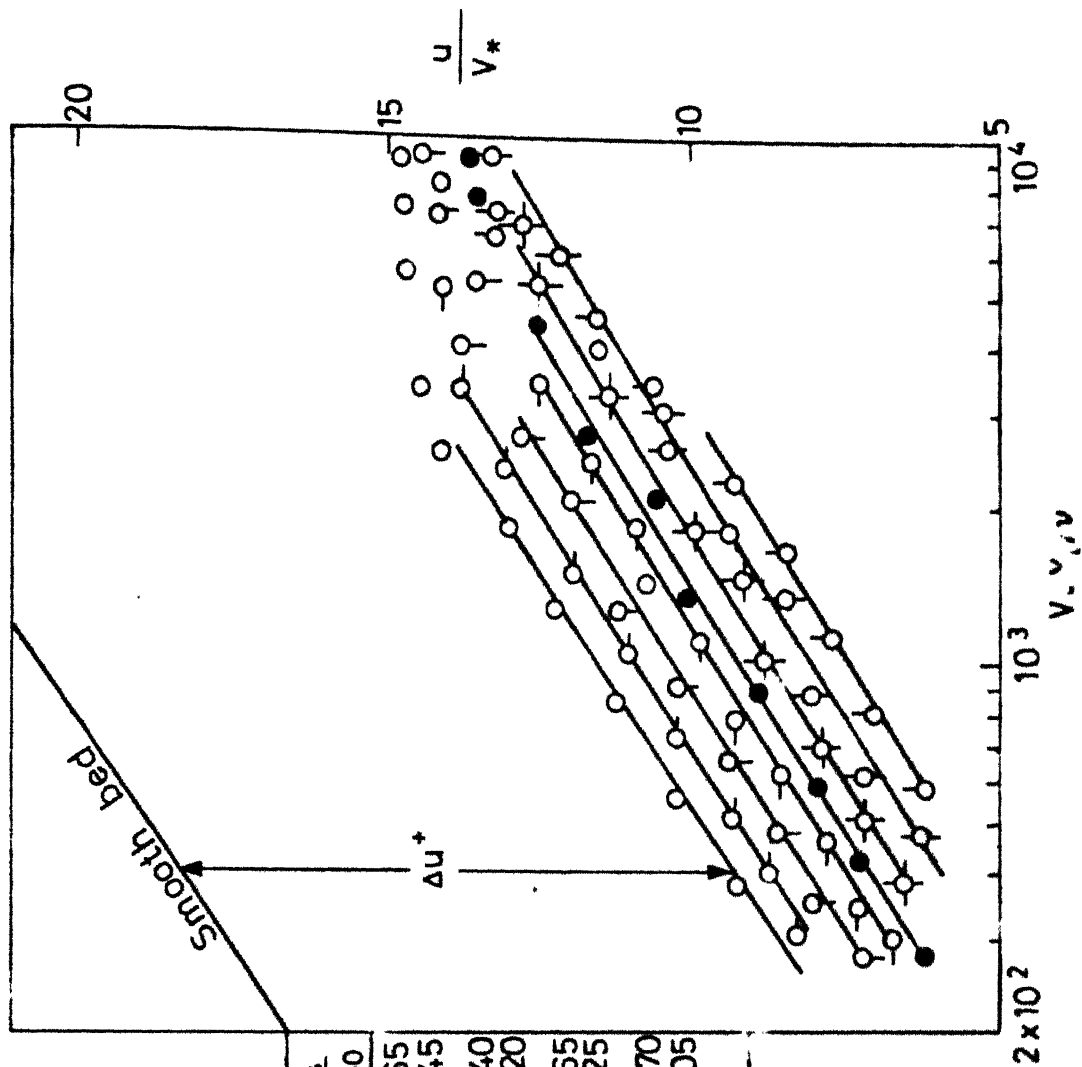


FIG.5 THE LAW OF WALL FOR SAND BED, NONUNIFORM IN SIZE, DENSELY PACKED 1.5 D SERIES

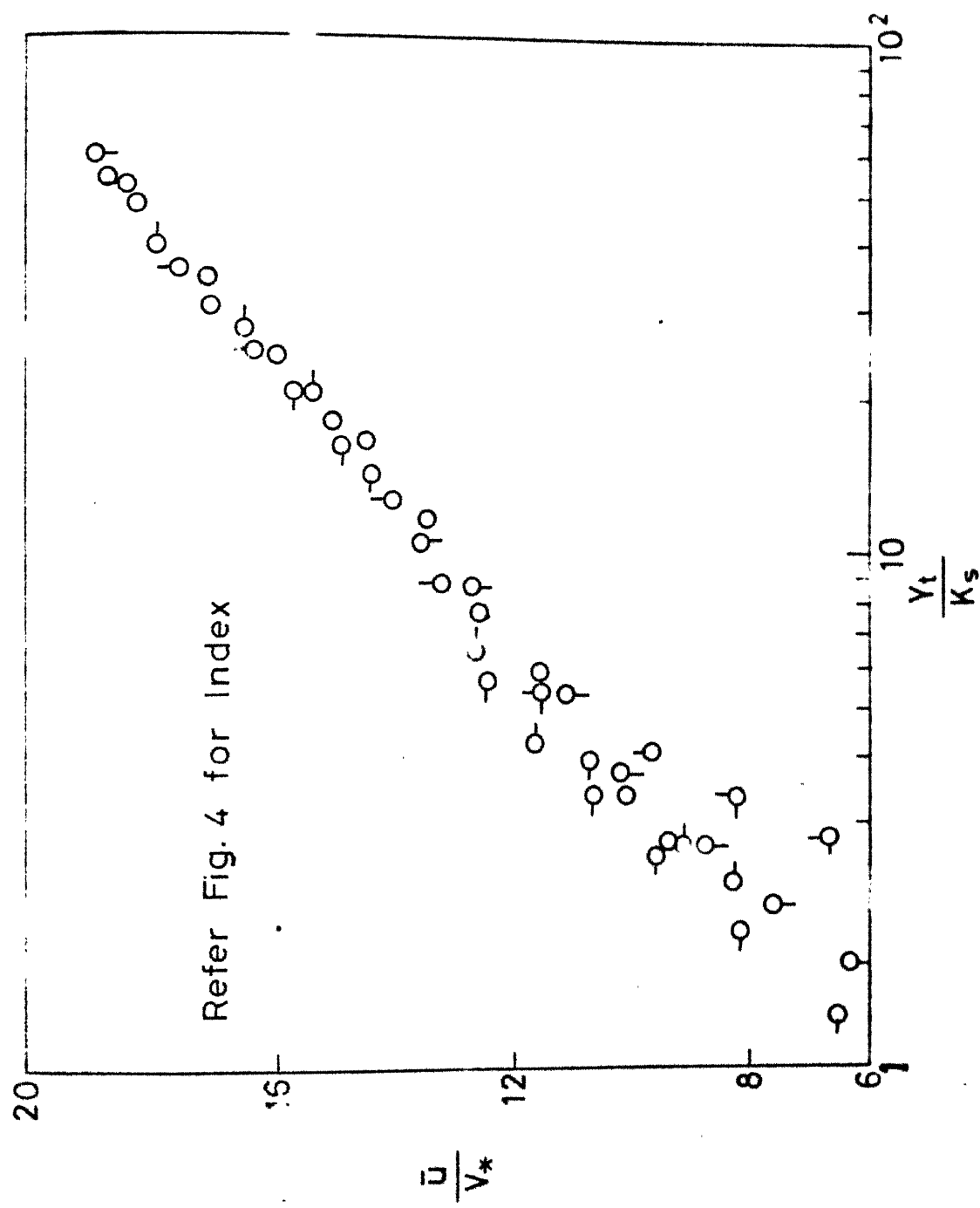


FIG 6 LAW OF WALL USING ROUGHNESS SCALE FOR 1.5 DS SERIES

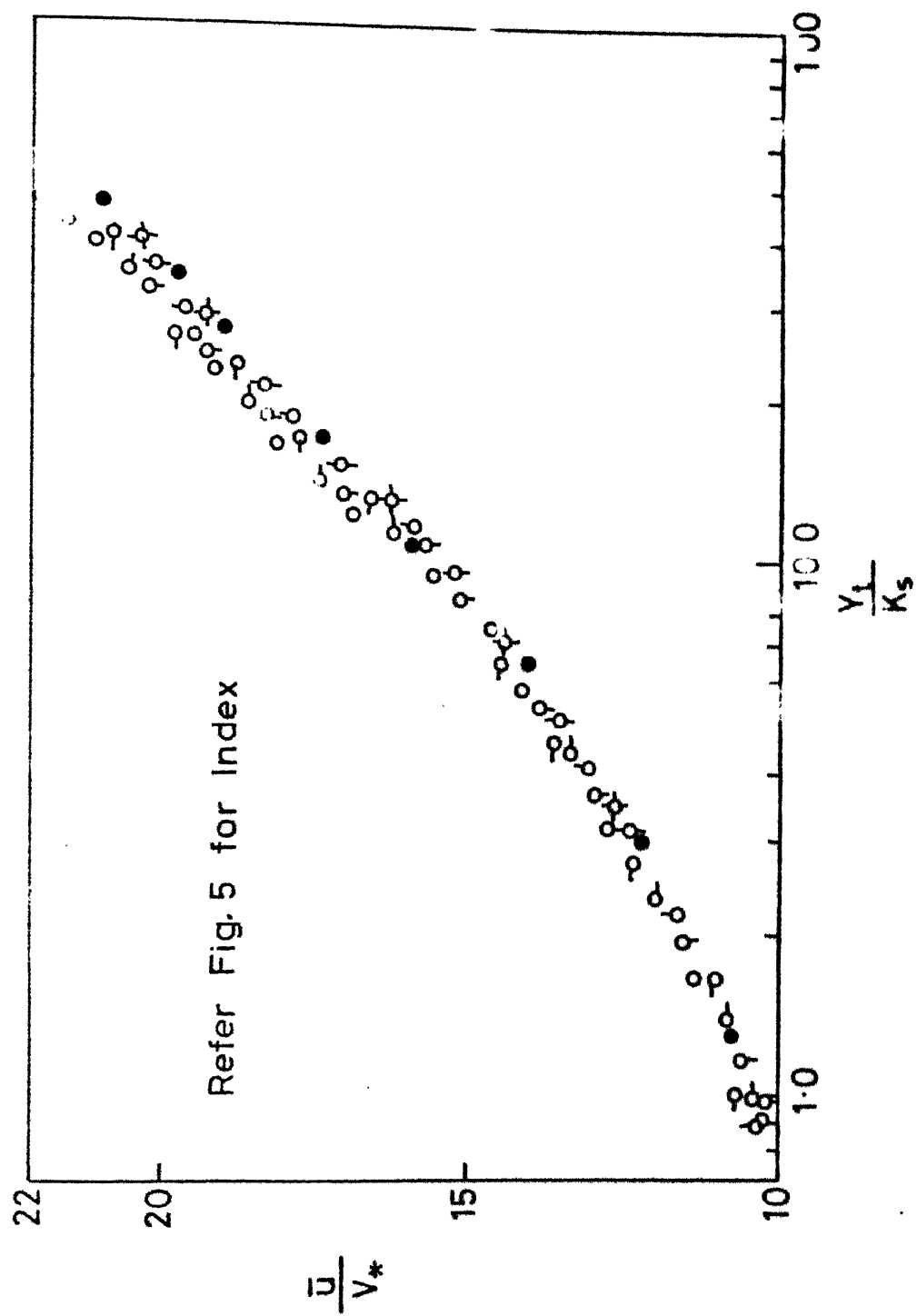


FIG.7 LAW OF THE WALL USING ROUGHNESS SCALE FOR 1.5 D SERIES

forms is taken up later in this chapter.

(b) Velocity defect law

(i) $\frac{U_\infty - \bar{u}}{v_*}$ as a function of y_t/δ_t .

The velocity defect $\frac{U_\infty - \bar{u}}{v_*}$ against y_t/δ_t has been plotted in Figs. 8 and 9. The data follows reasonably a single curve for $y_t/\delta_t > 0.2$. This clearly indicates that the effect of wall roughness is absent in the **defect** law region. In the region $y_t/\delta_t < 0.2$, the curves follow different curves having the magnitude of B_* different for each case. This is considered due to effect of geometry of the rough bed surface.

C. Functional Relationships for Roughness of Sand Grain Beds

The roughness scales K_s and $\frac{\Delta u}{v_*}$ that were introduced in the velocity profiles were found to vary with the surface characteristics λ or ϵ/d_{50} of the bed and flow characteristics $\frac{v_* d_{50}}{\nu}$.

Roughness parameters for randomly arranged, uniform or nonuniform size roughness elements can be related functionally to flow properties and rough surface properties as

LIB. KANPUR
CENTRAL LIBRARY
No. A 70554

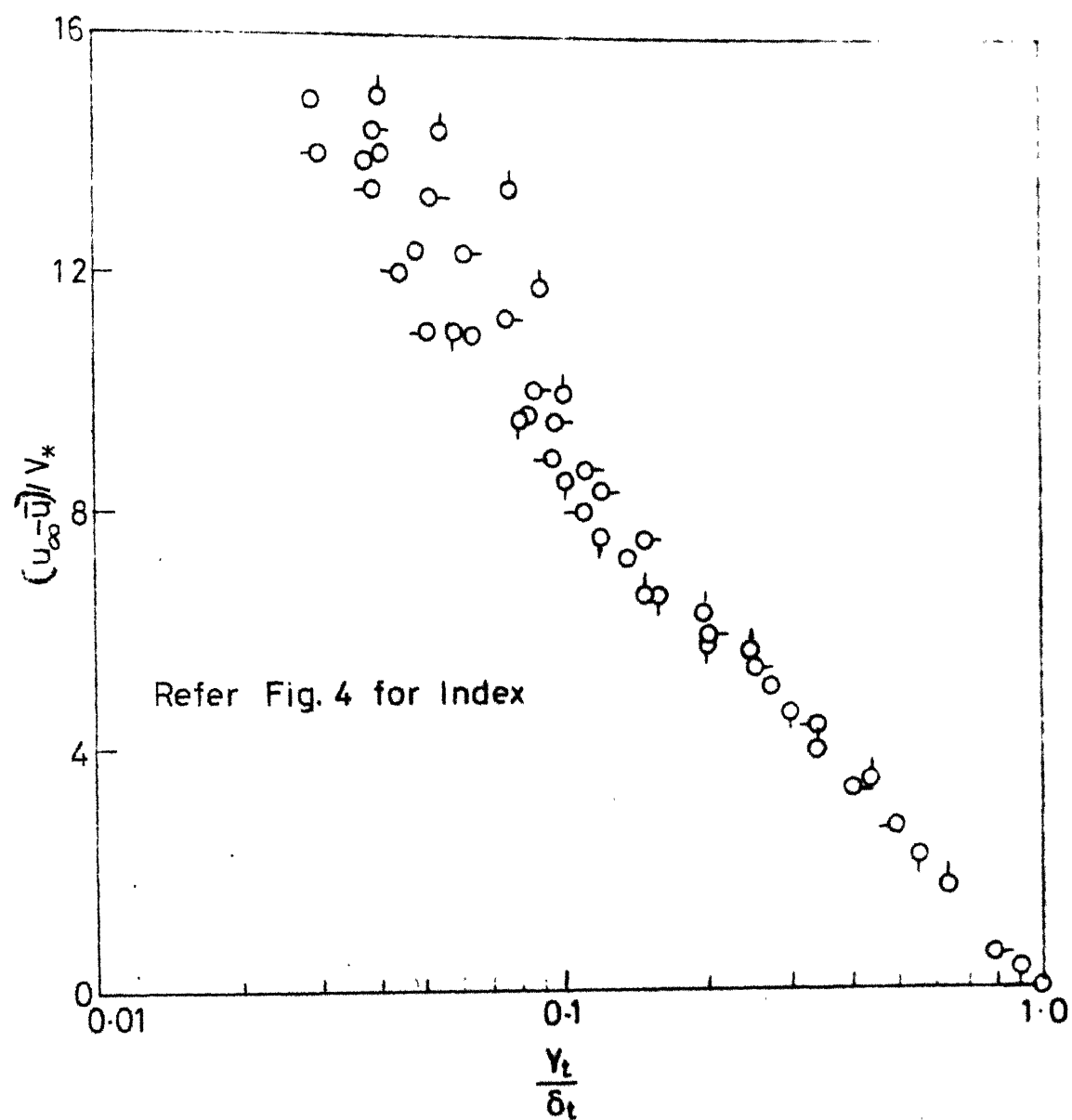


FIG. 8 VELOCITY DEFECT LAW FOR SAND GRAIN BEDS
(1.5 DS)

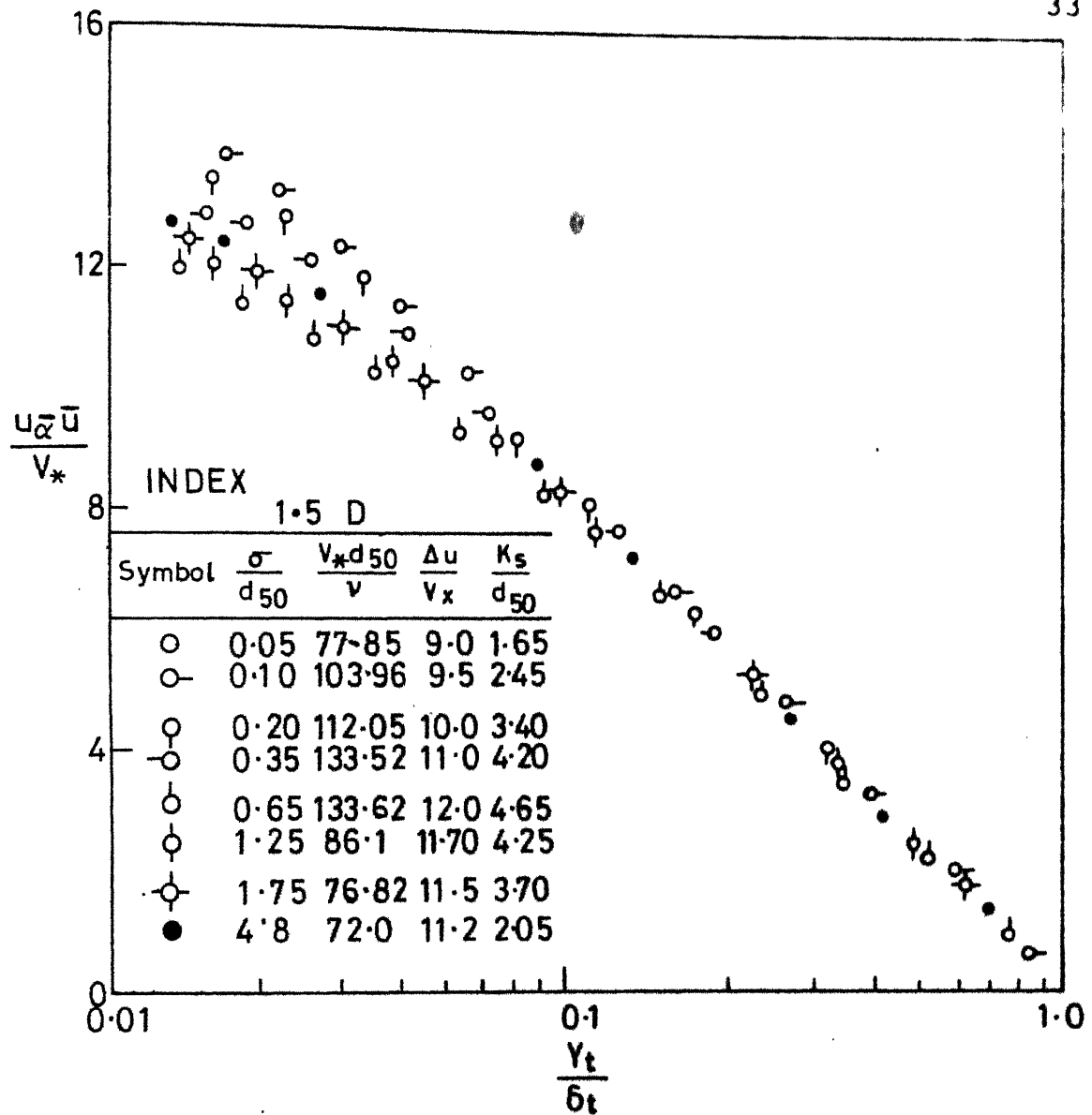


FIG. 9 VELOCITY DEFECT LAW FOR SAND GRAIN BEDS (1.5 D)

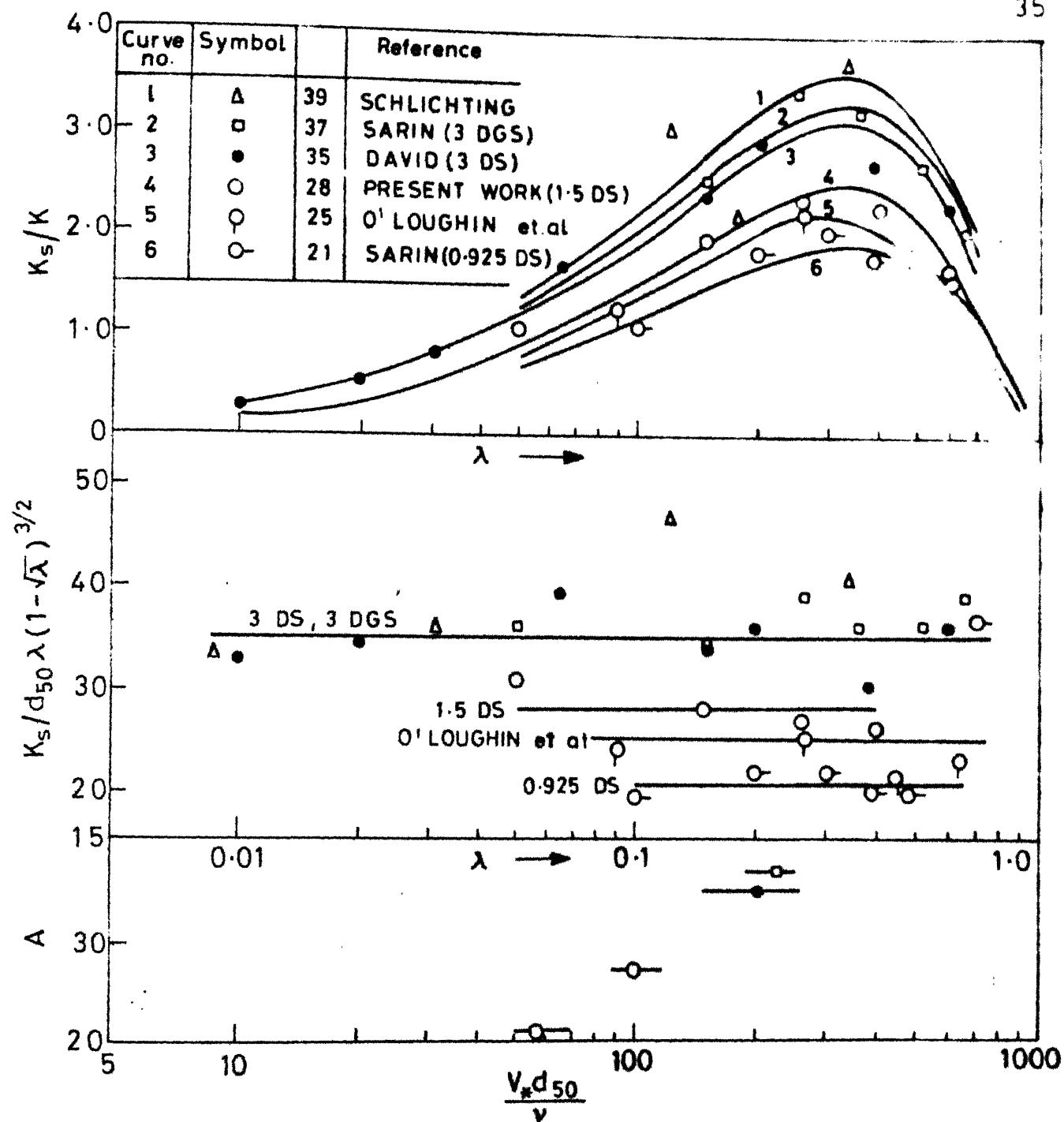
$$\left(\frac{\tau_s}{d_{50}}, \frac{\Delta u}{v_*} \right) = f \left(\frac{v_* d_{50}}{\nu}, \frac{C}{d_{50}}, \lambda \right)$$

Relationship of these parameters with roughness concentration and nonuniformity parameter C/d_{50} are discussed in detail in the following subsections.

(a) Effect of concentration on roughness of uniform sand grains randomly distributed

(i) Nikuradse's equivalent sand grain roughness (K_s):

The total effect of roughness of a surface can be represented by a single roughness scale K_s . The roughness scale parameter K_s/d_{50} is plotted against λ in Fig. 10. The results reported by Schlichting (1936), O'Loughlin et al. (1964), David (1980) and Sarin (1980) have also been plotted. For all these cases, it is seen that the value of K_s/d_{50} increases with λ , attains a maximum value at $\lambda = .25$ and then decreases with further increase in λ . David and Sarin have shown that for $\lambda < 0.1$, K_s/d_{50} varies linearly with λ , the constant of proportionality is function of $\frac{d_{50} v_*}{\nu}$. For values $\lambda > 0.1$, roughness scale decreases. The functional form of K_s/d_{50} with λ may be written as

FIG.10 EFFECT OF ROUGHNESS CONCENTRATION ON K_s

$$\frac{K_s}{d_{50}} = 1.4 \lambda (1.4 \lambda)^{3/2} \quad (15)$$

The proportionality constant 1.4 is a function of λ and λ varies with $d_{50} V_*$. Equation 15 agrees with experimental results fairly well as indicated in Fig. 10.

(ii) Shift in velocity scale $\Delta u/V_*$

The roughness scale represented as shift in velocity scale Δu is function of geometry of the roughness surface (λ) and flow properties like $\frac{d_{50} V_*}{\nu}$. David and Zirin showed that for constant surface geometry (λ), the $\frac{\Delta u}{V_*}$ increases linearly with increase in $\frac{1}{\lambda} \ln \frac{d_{50} V_*}{\nu}$. Hence, the function $\frac{\Delta u}{V_*} - \frac{1}{\lambda} \ln \frac{d_{50} V_*}{\nu}$ is supposed to be function of the geometry. This function is plotted against λ in Fig. 11. It may be noted that $\frac{\Delta u}{V_*} - \frac{1}{\lambda} \ln \frac{d_{50} V_*}{\nu}$ decreases on either side of $\lambda = 0.25$, similar to the variation of K_s/d_{50} with λ . The position of occurrence of peak values coincide for all cases with $\lambda = 0.25$, however, the magnitudes of peak values differ in each case. It may be observed that magnitudes of peak values $\frac{\Delta u}{V_*} - \frac{1}{\lambda} \ln \frac{d_{50} V_*}{\nu}$ for 3 DS, 1.5 DS and 0.915 DS vary slightly. This variation may be taken as experimental

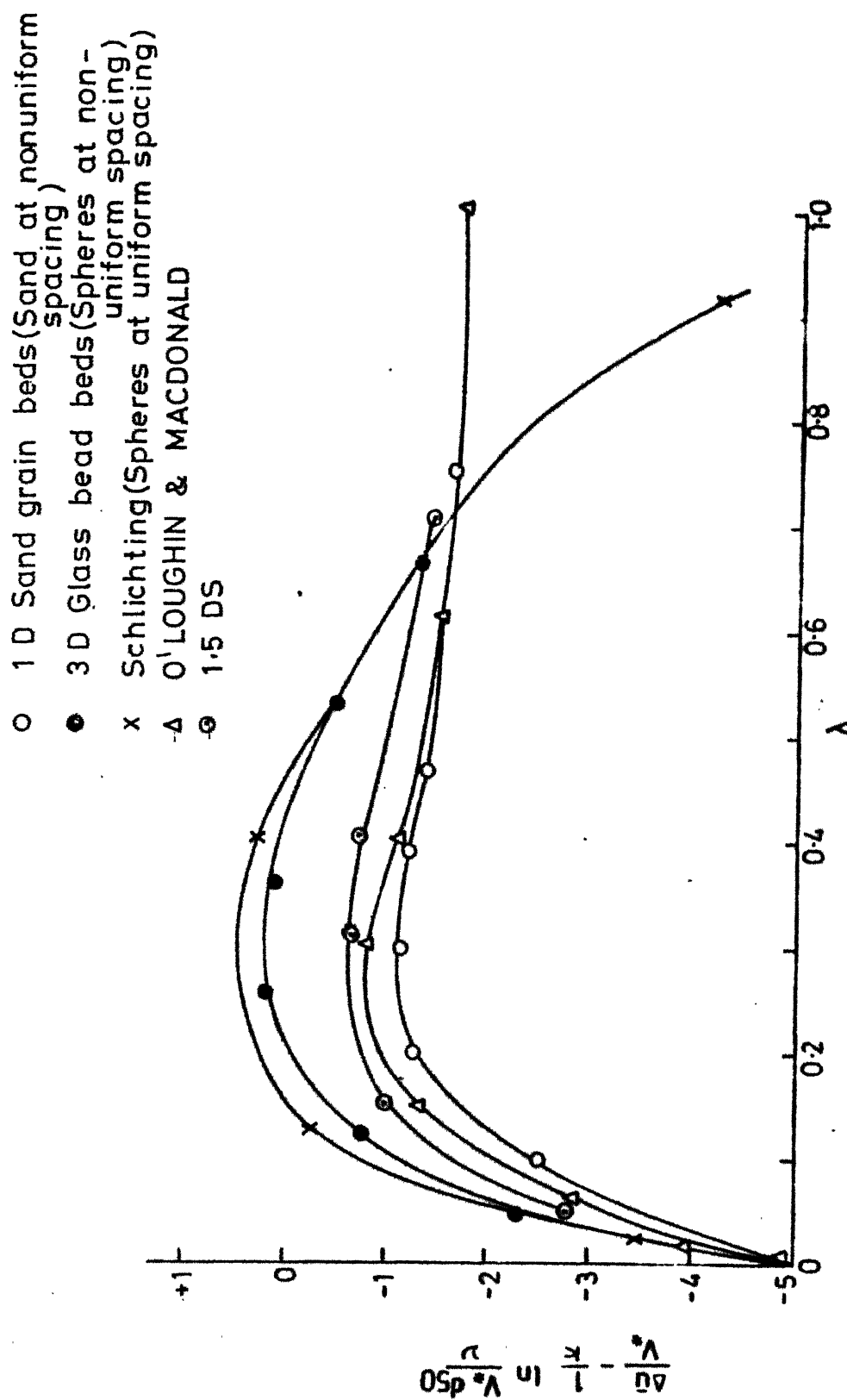


FIG. 11 EFFECT OF ROUGHNESS CONCENTRATION, ON LAW OF WALL INTERCEPT

scatter. The difference in peak values of glass beads (David and Schlichting data) is due to regularity in shape and arrangement pattern. The difference in peak values of 3D glass beads data Sarin, is indicative of regularity in shape and randomness in arrangement pattern. The present results adds the findings of Sarin that irregularity in shape and arrangement pattern decreases the roughness scale $\frac{\Delta u}{V_*} = \frac{1}{\lambda} \ln \frac{d_{50} V_*}{\nu}$, for $\lambda < 0.7$.

(iii) Theoretical bed level z/d_{50}

Theoretical bed level (3) is referred to as the location of the apparent origin for velocity distribution above the smooth surface of the flat bed.

The plot of z/d_{50} against λ is shown in Fig. 12. It is observed that the theoretical bed level shifts from the top of the grains towards its bottom as the roughness concentration of the bed decreases for 3DS sand bed series. For 0.925 DS and 1.5 DS sand bed series, z/d_{50} is greater than one, indicating that the theoretical bed level lies above d_{50} level. This is due to predominance of viscosity effect in these sand bed series.

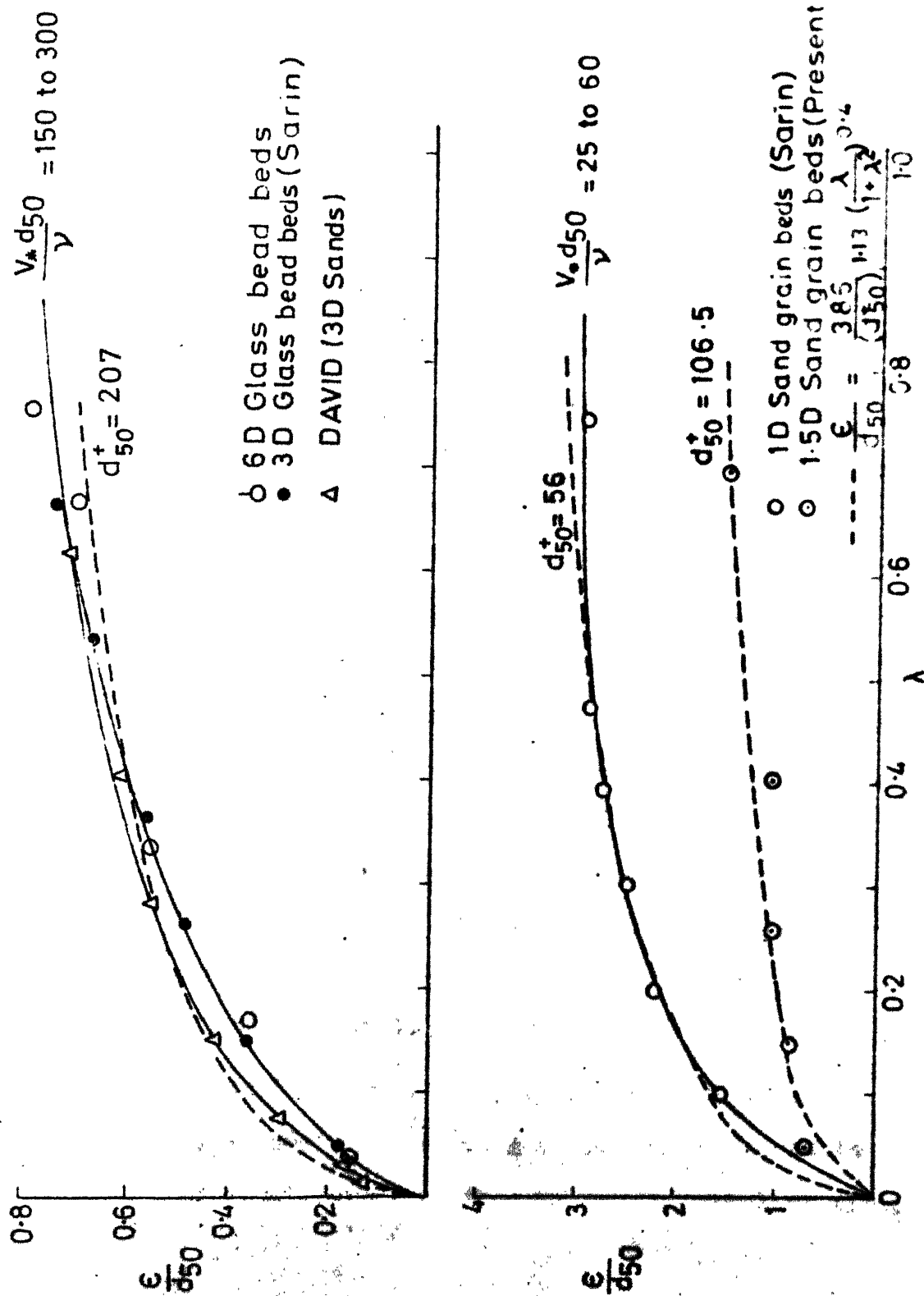


FIG.12 EFFECT OF ROUGHNESS CONCENTRATION ON THEORITICAL BED LEVEL

- (b) Effect of nonuniformity in grain size on the Roughness of sand beds densely covered by the grains
- (i) Nikuradse's roughness function K_s/d_{50}

Nikuradse's roughness function K_s/d_{50} is plotted against nonuniformity parameter δ/d_{50} for data of 1.5 D along with those of P.K. Mittal, S. Mittal and David in Fig. 13. It is observed that as nonuniformity δ/d_{50} increases, roughness function K_s/d_{50} also increases, attains a peak value and then decreases with further increase in

δ/d_{50} . The value of δ/d_{50} at which maximum K_s/d_{50} occurs varies with the range of $\frac{V_* d_{50}}{\nu}$. For $\frac{V_* d_{50}}{\nu} > 200$, $\frac{K_s}{d_{50}}$ has a unique curve for δ/d_{50} , whereas it gives different curves for $\frac{V_* d_{50}}{\nu} < 200$. The slope of the rising limbs of these curves gradually decreases with the decrease in $\frac{V_* d_{50}}{\nu}$, and that of the receding limbs remains constant. The peak values of all the bed series are fairly constant. The present experimental results covers the wide gap left between the data of David and P.K. Mittal and S. Mittal.

The shift in curves of K_s/d_{50} with δ/d_{50} for different d_{50} may be attributed to change in the state of flow from rough turbulent flow to smooth turbulent flow.

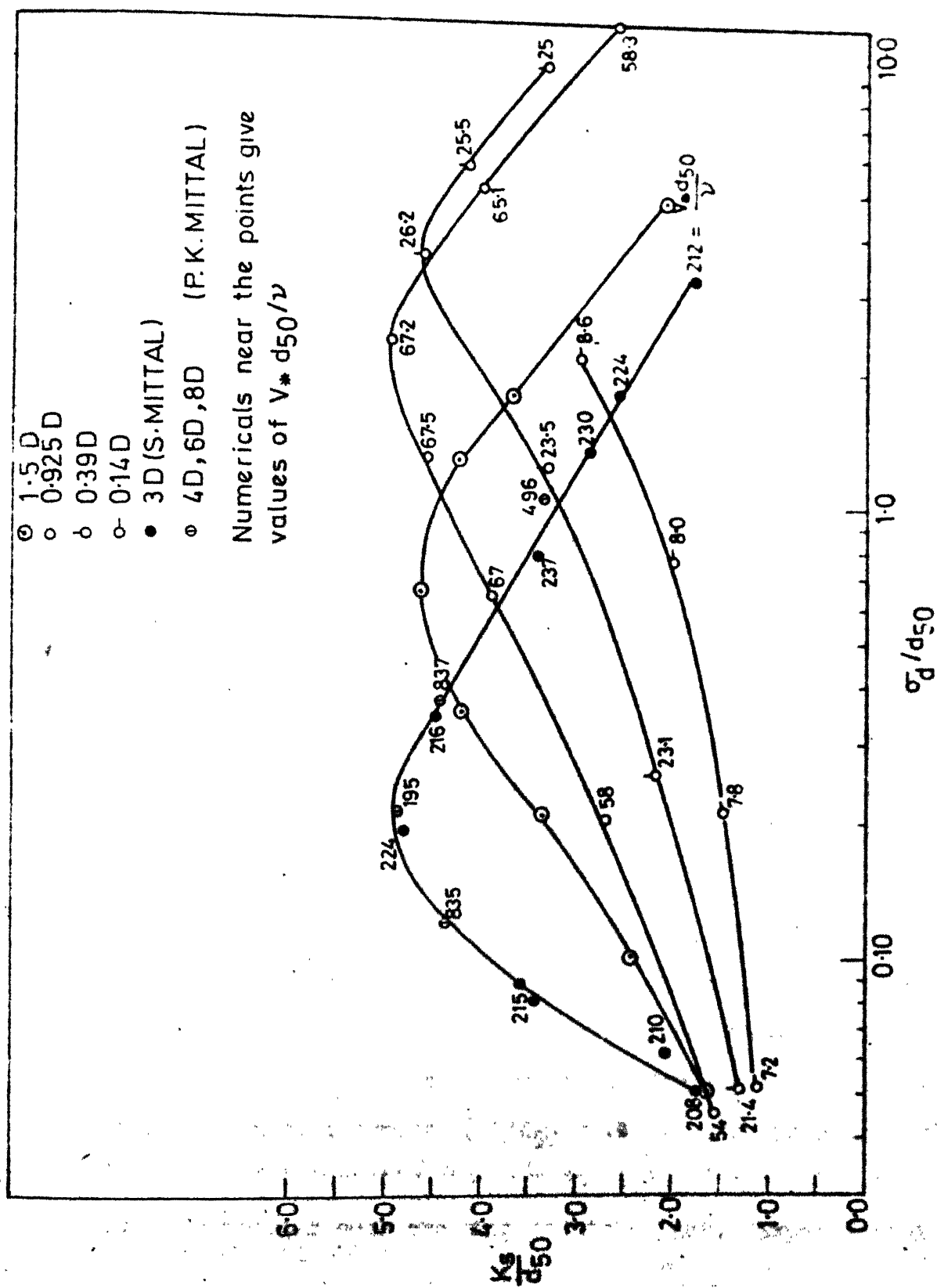
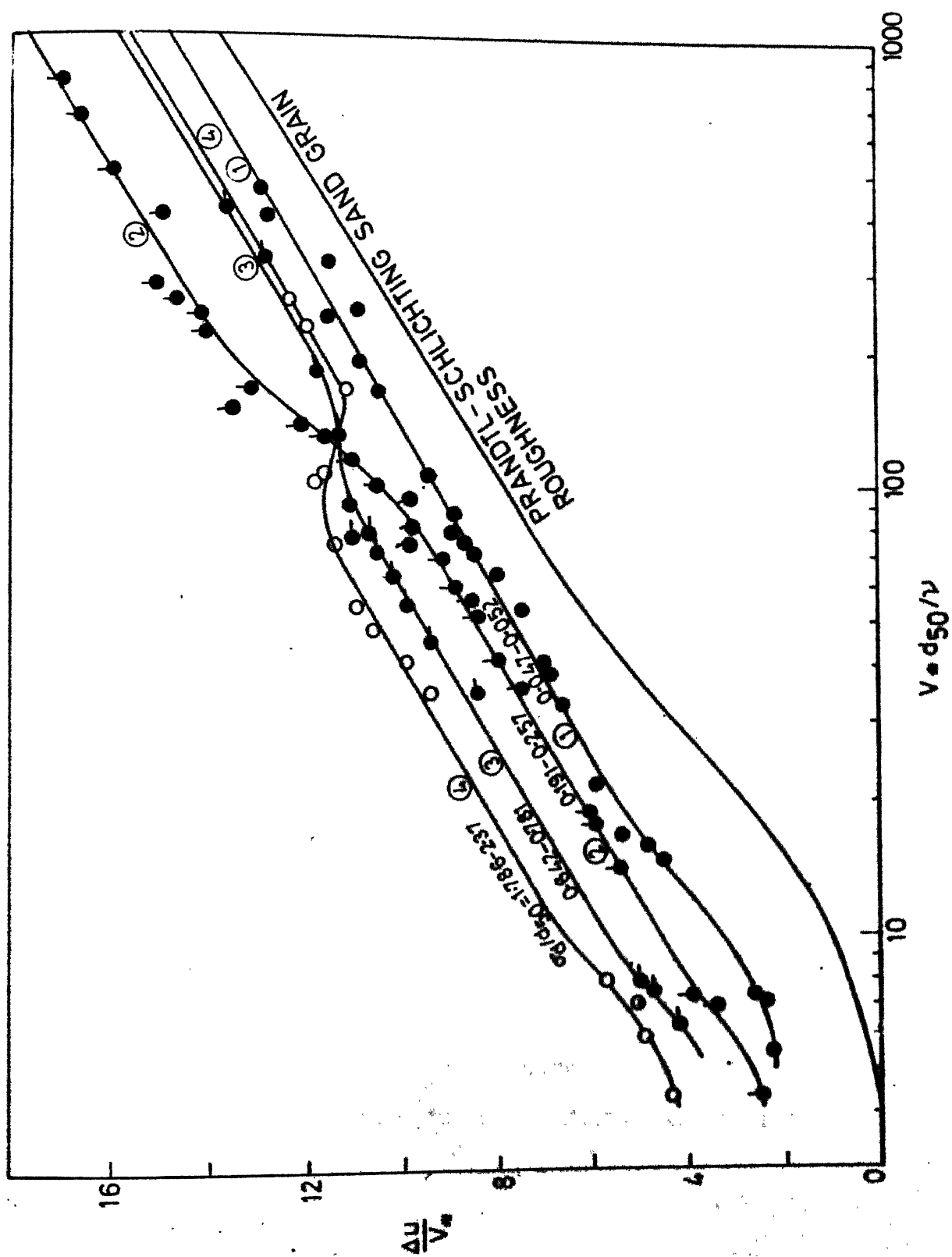


FIG. 13 EFFECT OF NONUNIFORMITY IN GRAIN SIZE ON EFFECTIVE ROUGHNESS SCALE K_s

However, it may be noted that region of rough turbulent zone exists for $\frac{v_* d_{50}}{\nu} > 200$, whereas from Nikuradse's experiments it is in the region $\frac{d_{50} v_*}{\nu} > 70$. The region for $5 < \frac{d_{50} v_*}{\nu} < 70$ is a transition region according to Nikuradse, in the present case the region is for $\frac{d_{50} v_*}{\nu} < 200$.

(ii) Shift in velocity scale $\frac{\Delta u}{v_*}$

The effect of roughness can also be expressed as the vertical shift $(\frac{\Delta u}{v_*})$ in the velocity distribution from smooth wall to rough wall. The velocity shift $\frac{\Delta u}{v_*}$ is plotted against $\frac{v_* d_{50}}{\nu}$ for nonuniform sand grain beds using present experimental results along with the data of David and S. Mittal as shown in Fig. 14. It may be observed that data of certain range of nonuniformity σ/d_{50} follow a particular curve. The region above $\frac{v_* d_{50}}{\nu} > 200$, and region $20 < \frac{v_* d_{50}}{\nu} < 70$ follow a straight line variation on semilog plot with slope equal to $1/\kappa$. In region $\frac{v_* d_{50}}{\nu} < 20$, curves drop down, indicating towards the region of smooth turbulent flow. In the region $70 < \frac{v_* d_{50}}{\nu} < 200$ the curves cross each other except for curve having low value of nonuniformity ($\sigma/d_{50} = .05$). The present experimental investigation was carried out specially to verify whether such crossing exists or not. Experimental



results do prove the existence of crossing of the curves. This phenomena is due to shift of roughness scale curves due to viscosity. Roughness scale models were developed subsequently.

The functional form $\Delta u^+ - \frac{1}{\alpha} \ln d_{50}^+$ is supposed to be independent of $\frac{d_{50} v_*}{\nu}$ and functions of σ/d_{50} only. In order to study this variation $\Delta u^+ - \frac{1}{\alpha} \ln d_{50}^+$ is plotted against σ/d_{50} as shown in the Fig. 15. It is observed that as nonuniformity σ/d_{50} increases,

$\Delta u^+ - \frac{1}{\alpha} \ln d_{50}^+$ increases, reaches a peak value and then decreases with further increase in σ/d_{50} . The value of σ/d_{50} at which maximum $\Delta u^+ - \frac{1}{\alpha} \ln d_{50}^+$ occurs varies with the range of $\frac{v_* d_{50}}{\nu}$, for $\frac{v_* d_{50}}{\nu} > 200$, $\Delta u^+ - \frac{1}{\alpha} \ln d_{50}^+$ has a unique curve for σ/d_{50} , whereas it gives different curves for $\frac{v_* d_{50}}{\nu} < 200$. The peak values of $\Delta u^+ - \frac{1}{\alpha} \ln d_{50}^+$ remains fairly same for each range of $\frac{v_* d_{50}}{\nu}$.

The present experimental result covers the wide gap between the data of P.K. Mittal, S. Mittal and David.

Existence of unique curve for $d_{50}^+ > 200$ may be attributed to rough turbulent flow. As the flow changes from

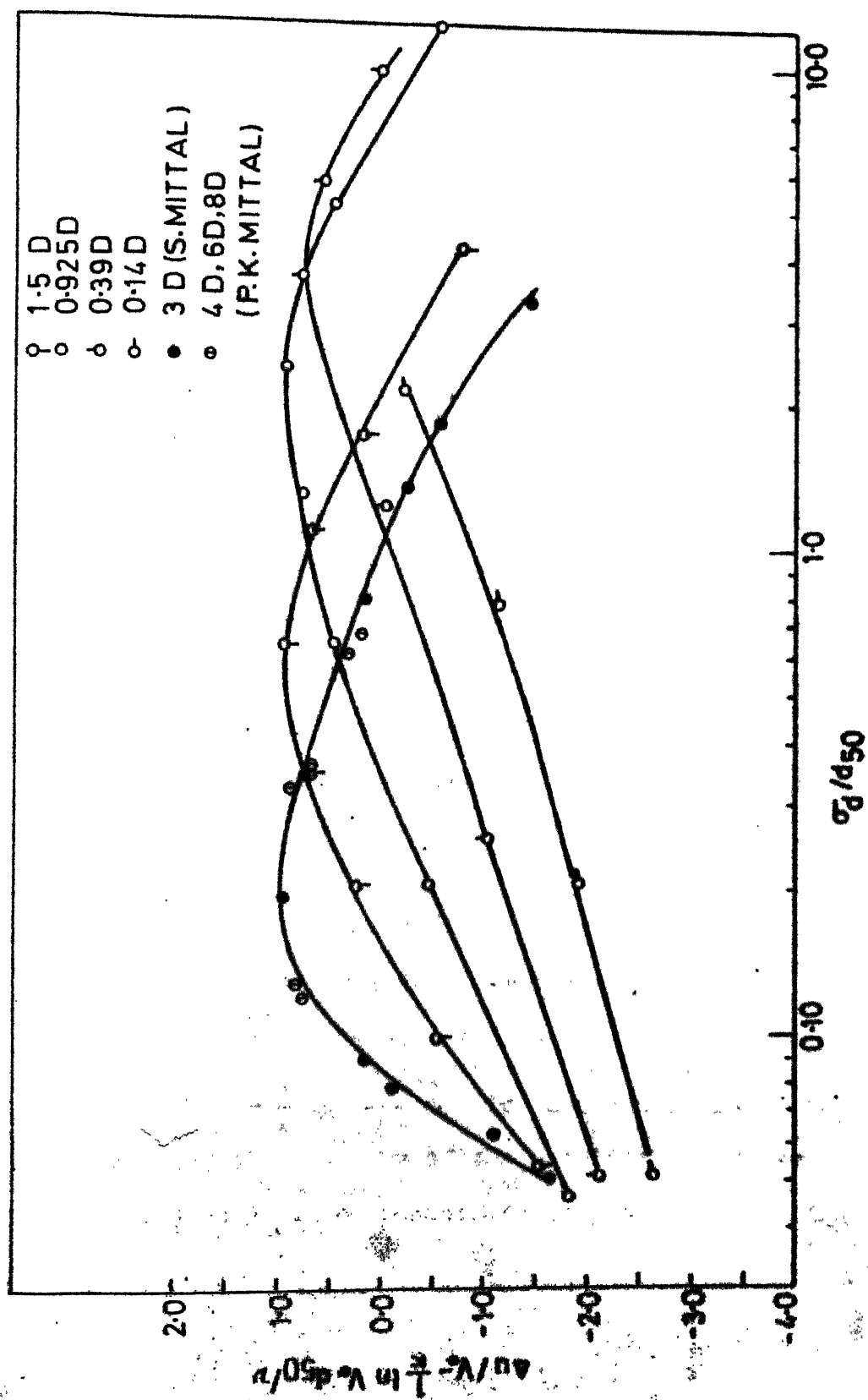


FIG. 15 EFFECT OF NONUNIFORMITY IN GRAIN SIZE ON THE LAW OF THE WALL INTERCEPT

rough turbulent to smooth turbulent flow, the curves shift with particular values of Grain Shear Reynolds number.

(iii) Theoretical bed level z/d_{50}

Theoretical bed level ' z ' is measured from the flat surface on which the sand grains are stuck. The magnitude, z/d_{50} is found to vary in particular way for given $\frac{V_* d_{50}}{\nu}$, as shown in Fig. 16. The value of z/d_{50} is maximum for $\epsilon/d_{50} = 0.05$ and decreases with increase in ϵ/d_{50} . Experiments reported in literature also indicate the value of $z/d_{50} = 0.75$. However, in the present investigation and investigation carried out by David, z was found to lie above d_{50} level in many cases. This effect may be attributed to low values of $\frac{d_{50} V_*}{\nu}$ or transition from rough turbulent flow to smooth turbulent flow.

D. Model for Roughness Scale

From the study made in previous paragraphs, it was shown that roughness scales represented in the form of $\frac{K_s}{d_{50}}$ or $\Delta u^+ = \frac{1}{\kappa} \ln \frac{d_{50} V_*}{\nu}$ is function of parameters representing the geometry of the bed like roughness concentration λ , and nonuniformity parameter ϵ/d_{50} and

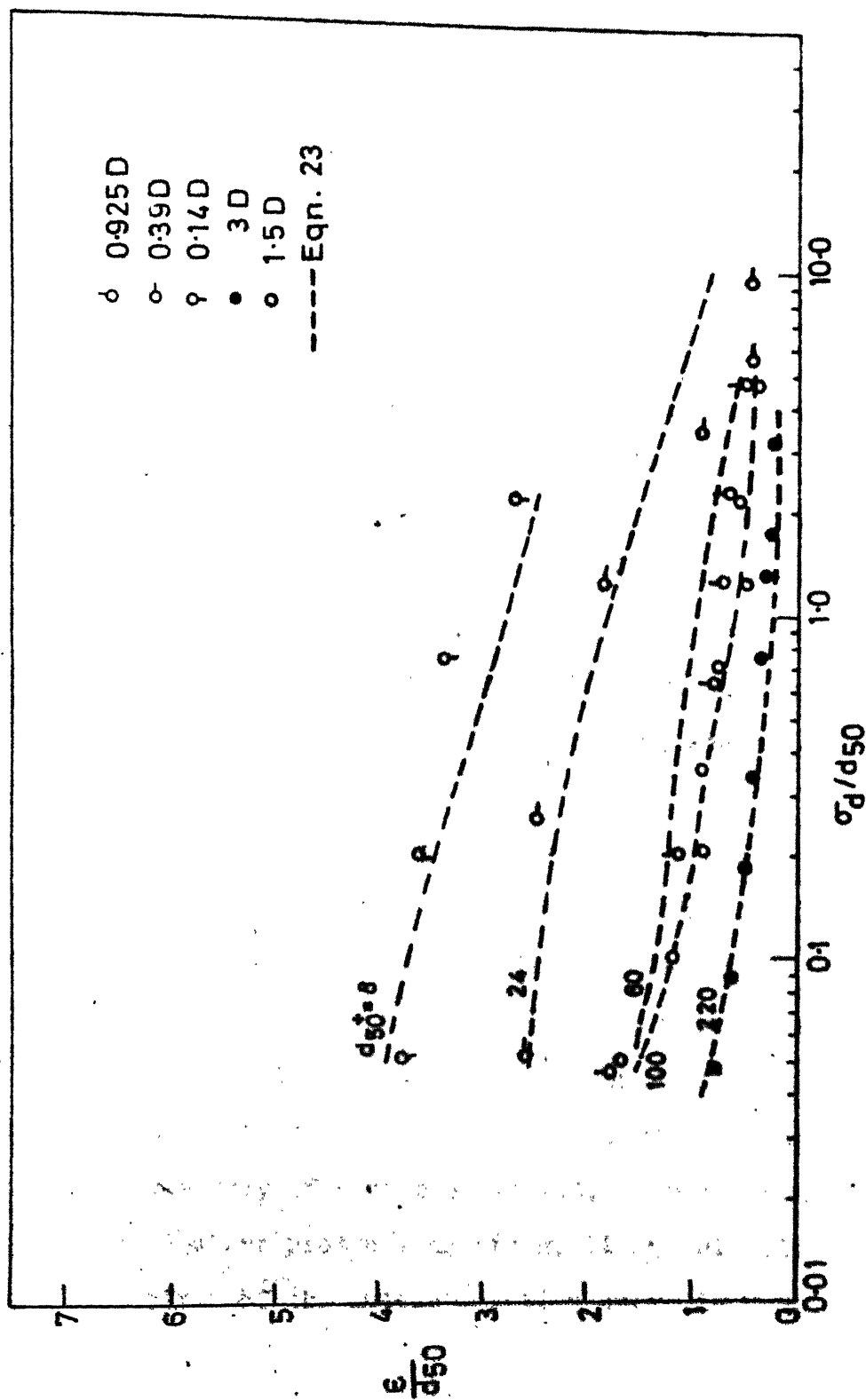


FIG. 16 EFFECT OF NONUNIFORMITY IN GRAIN SIZE ON THE THEORETICAL BED LEVEL

parameter representing the state flow namely Gravitational Shear Reynolds number, $\frac{d_{50} V_*}{\nu}$. A model for roughness scales in terms of above parameters has been attempted in the following paragraphs.

(a) Model based on the geometry of the rough bed profile

From the literature study it was noted that a particular representative size for beds having nonuniform sand grain densely packed was chosen. To name the few such sizes are d_{50} , d_{65} and d_{90} . It was shown by David, P.K. Mittal and S. Mittal that along with particular size, it is necessary to use second statistical parameter namely standard deviation. Standard deviation 'σ' was found to give better representative geometric scale.

Standard deviation does not consider the persistence of occurrence of particular size. In order to include this characteristic, the autocorrelation and power spectral study of the sand grain protrusions is made. Typical plots of autocorrelation and power spectral density are shown in Fig. 17. It may be observed from the autocorrelation curve that the slope of the curve before zero crossing is function of geometry of sand bed profile. For uniform grains, densely packed where protrusions are small and closely spaced, the slope of the autocorrelation curve is very

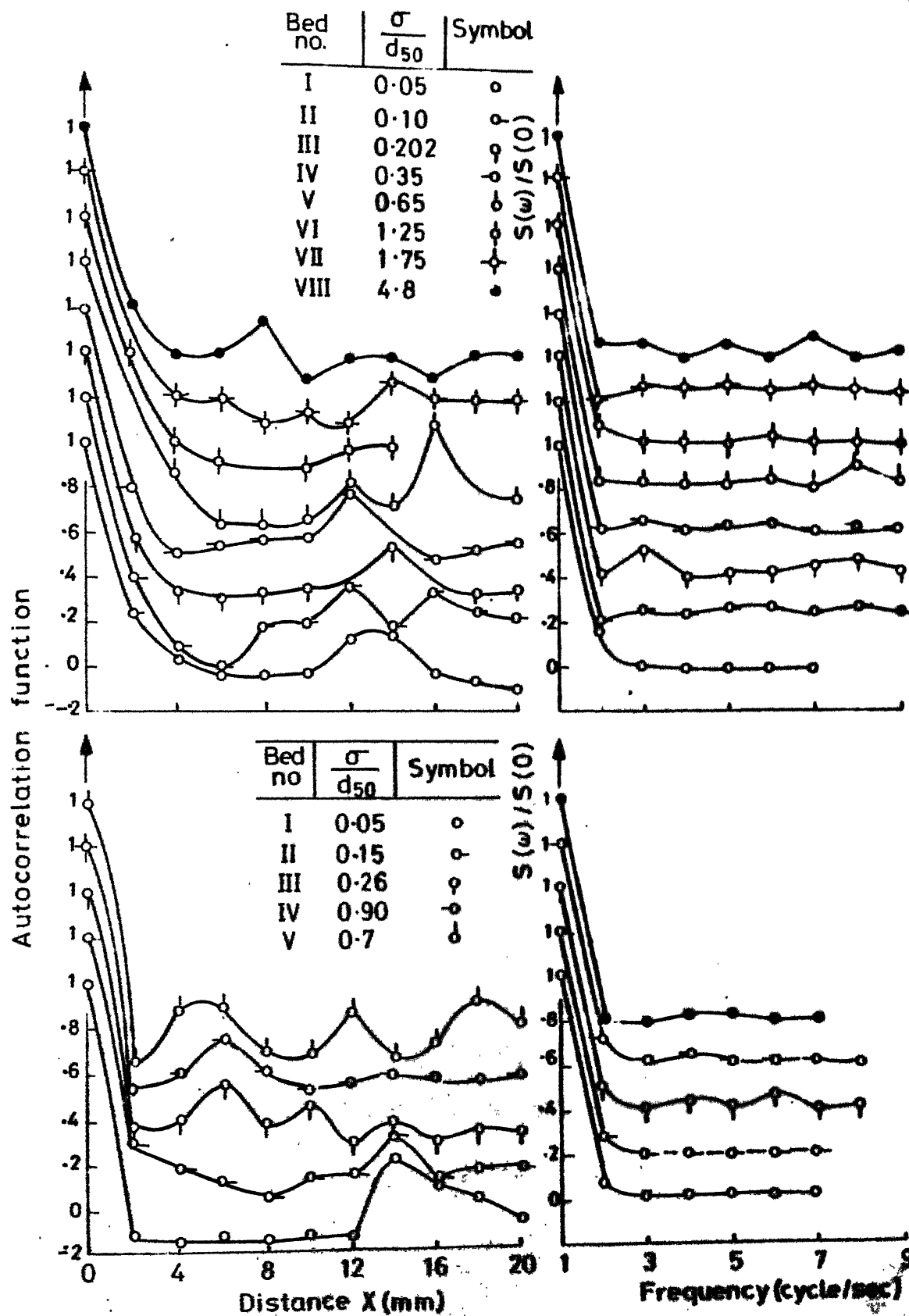


FIG.17 AUTOCORRELATION AND SPECTRAL DENSITY OF GRAIN HEIGHT FOR 1.5 DS AND 1.5 D BED SERIES

steep. As the protrusions size and spacing increase, the slope of the autocorrelation curve decreases. Hence, the slope of autocorrelation curve is considered to represent the spacing characteristic of sand grains on sand bed. In order to utilize this information the representation of geometric scale, the slope of autocorrelation curve denoted as 'Sa' was multiplied with the standard deviation ' σ ' and used in the study. Table 2 shows the values of $\frac{\sigma h S_a}{d_{50}}$ for different σ/d_{50} . From the study of the table it may noted that $\frac{\sigma h S_a}{d_{50}}$ remains fairly constant value for all the σ/d_{50} for a given bed series. This constancy character donot represent the characteristics variation of roughness scales. Hence this approach is not considered for further analysis.

The sand surface is assumed to represent combination of number of irregular waves of certain height and spacing. The significant wave height can be considered to represent the one of the geometrical properties of irregular waves. This significant wave height H_s may be represented according to Cartwright and Longuet-Higgins (1965) as

$$H_s = 4.005 \sigma_h (1-m^2)^{1/2} \quad (16)$$

TABLE 2 : AUTOCORRELATION SLOPE VALUES

3D			.925 D		
$\frac{\sigma}{d_{50}}$	s_a	$\frac{\sigma_h s_a}{d_{50}}$	$\frac{\sigma}{d_{50}}$	s_a	$\frac{\sigma_h s_a}{d_{50}}$
.051	5.0	1.50	.047	2.5	1.04
.0804	4.25	1.40	.203	1.92	0.805
.0899	4.15	1.40	.642	1.47	0.85
.191	4.0	1.60	1.302	1.92	0.91
.339	3.22	1.40	2.37	0.80	0.92
.781	2.62	1.13	5.05	1.22	1.51
1.317	1.82	1.00	12.0	2.63	2.55
1.786	1.42	1.30	0.39D		
3.26	0.87	1.30	.052	3.57	1.47
1.55D			.257	1.40	0.67
.05	3.24	1.05	1.227	1.30	1.74
.10	3.0	1.20	3.593	2.0	3.26
.202	2.2	.90	5.629	1.25	2.19
.35	0.635	.95	9.567	.9	1.17
.65	0.67	1.12	0.14 D		
1.25	0.475	1.09	.052	1.61	.71
1.75	0.396	1.95	.208	1.79	.82
4.80	0.179	0.85	.766	3.125	3.48
			2.120	2.940	3.78

In which σ is standard deviation and m is defined as

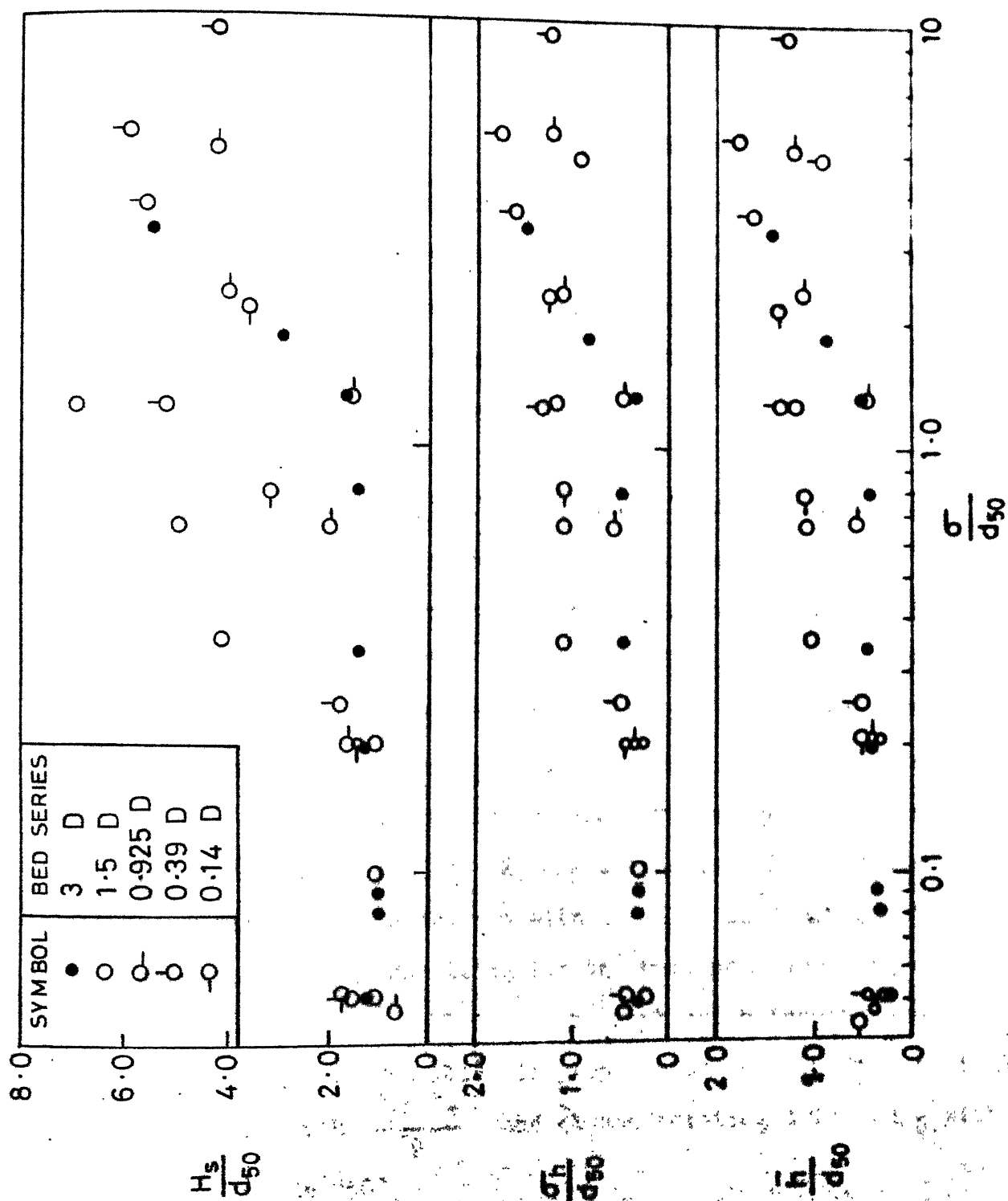
$$m = \left(1 - \frac{S_2^2}{S_0 S_4} \right)^{1/2}$$

where S_0 , S_2 and S_4 are zeroth, second and fourth spectral moments which in a general form can be represented as follows:

$$S_n = \int_0^\infty \omega^n S(\omega) d\omega \quad (17)$$

where $S(\omega)$ is the significant spectral density corresponding to frequency ω (in radians per second). The values of m computed by this formula are tabulated in appendix.

Using this computed values of σ and m , the significant height of sand surface protrusions was computed and is plotted in Fig. 18. It may be observed that this significant height in the form H_s/d_{50} increases with increase in σ/d_{50} attains a maximum value and then decreases with further increase in σ/d_{50} . This variation is similar to the variation of K_s/d_{50} with σ/d_{50} . Variation of σ_H/d_{50} and H/d_{50} with σ/d_{50} in the Fig. 18. Nonuniformity parameter based as protrusions height namely σ_H/d_{50} increases with nonuniformity parameter σ/d_{50} upto certain value and then after starts decreasing with increase in σ/d_{50} . This variation is not observed in all the series of beds. The

FIG.18 VARIATION OF SIGNIFICANT HEIGHT WITH σ/d_{50}

mean height of protrusions \bar{h}/d_{50} increase with increase in σ/d_{50} attains certain maximum value and then decreases with further increase in σ/d_{50} . This variation is consistently observed for all the sand bed series.

From these geometrical model study, it may be observed that the state of flow has to be taken into consideration in analysis. With this as aim, the following models are developed for uniform grain randomly spaced and for nonuniform grains densely packed.

(b) Model for Roughness of uniform grains randomly spaced

Roughness of uniform sand grains randomly spaced was experimentally investigated by David for $d_{50} = 3.0$ mm, Sarin for $d_{50} = 0.925$ mm and $d_{50} = 1.5$ mm during present investigation. In all these investigations the following common features are observed. The maximum value of roughness scale like K_s/d_{50} occurs at or around roughness concentration $\lambda = 0.26$ and either side this value of λ , K_s/d_{50} decreases. The magnitude of the maximum value decreases with decrease in Grain Shear Reynolds number. Modelling for the roughness scale K_s/d_{50} is proposed in the following per graph which incorporates above features. Modelling is proposed by relating theoretical bed θ/d_{50} with $\frac{d_{50} V_*}{\nu}$ and λ and relating this θ/d_{50} with τ_{Au}^+ and K_s/d_{50} .

Theoretical bed level z/d_{50} is plotted against roughness concentration λ as shown in Fig. 12. It was observed that the experimental values of z/d_{50} with λ follow a separate parallel curves for each median size namely 3.0 mm, 1.5 mm and 0.925 mm. These curves are interrelated with Grain Shear Reynolds number $\frac{V_* d_{50}}{\nu}$ as shown in Fig. 12 using an empirical equation given below

$$\frac{z}{d_{50}} = -\frac{386}{\left(\frac{d_{50} V_*}{\nu}\right)^{1.13}} \left(\frac{\lambda}{1+\lambda^2}\right)^{0.4} \quad (18)$$

The roughness scale represented in terms of shift in velocity and theoretical bed level are found to be related with λ and $\frac{d_{50} V_*}{\nu}$ as

$$\Delta u^+ = \frac{1}{2} \ln e^+ = 1.5 - \text{Exp. } 0.00535(20 + \xi)^{1/3}(110 - \xi) \quad (19)$$

where $e^+ = \frac{2V_*}{\nu}$ and $\xi = (\sqrt{\lambda} + \sqrt{(1-\lambda)\sqrt{\lambda}})(1-\lambda)\frac{d_{50}V_*}{\nu}$

Here the parameter ξ represents the sum of mean height and standard deviation of heights as

$$\xi = \left(\frac{\bar{h}}{d_{50}} + \frac{\sigma_h}{d_{50}} \right) (1-\lambda) \frac{d_{50}V_*}{\nu} \quad (20)$$

Using the above functions, the relation for shift in the velocity scale is written as

TABLE 3 : COMPUTED ROUGHNESS SCALE VALUES

3 DS			1.5 DS			0.925 DS		
λ	K_s/d_{50}		λ	K_s/d_{50}		λ	K_s/d_{50}	
	Exptt.	Computed		Exptt.	Computed		Exptt.	Computed
.01	.28	.3744	.05	1.05	1.0973	.10	1.1	1.66
.02	.55	.6588	.15	2.0	2.29	.20	1.85	2.32
.065	1.70	1.4735	.26	2.40	2.84	.30	2.05	2.66
.150	2.45	2.2500	.40	2.33	2.77	.39	1.80	2.645
.262	2.95	2.5100	.70	1.72	1.47	.47	1.65	2.228
.394	2.70	2.9680				0.75	1.25	2.210
.608	2.30	2.2400						

$$\Delta u^+ - \frac{1}{x} \ln d_{50}^+ = \frac{1}{x} \ln \left(\frac{386}{\left(\frac{d_{50}^+}{\lambda} \right)^{1.13}} \right) \lambda^{0.4} + 1.5 - \text{Exp}(0.00535(20 + \xi)^{1/3}(110 - \xi)) \quad (21)$$

The roughness scale K_s/d_{50} is related with above equation using the equations 9 and 21 as

$$\frac{K_s}{d_{50}} = - \frac{3.3}{d_{50}^+} + \frac{3.215 \times 386}{(d_{50}^+)^{1.13}} \text{Exp} \left[\left\{ 1.5 - \text{Exp}.00535(20 + \xi)^{1/3} \right. \right. \\ \left. \left. (110 - \xi) \right\} \right] \quad (22)$$

Using the average d_{50}^+ values for these three bed series the value of K_s/d_{50} is calculated and tabulated along with experimental values in table 3 shown below. The computed values of K_s/d_{50} are consistently higher in comparison to experimental values. The maximum value of K_s/d_{50} occurs around $\lambda = 0.3$.

c. Model for Roughness of sand beds having nonuniform sand grains densely packed

Experimental results of series of sand beds with 1.5 mm as median diameter of the present work, and the data of P.K. Mittal, S. Mittal and David for sand bed series for different median grain diameters ranging from 8.0 mm to 0.14 mm are used in the development of model for sand

beds with nonuniform sand grains densely packed. From the experimental data, referring to Fig. 13, the following observations may be noted. The magnitude of K_B/d_{50} increases with increase in σ/d_{50} , attains a maximum value and with further increase in σ/d_{50} , it decreases. The position at which maximum value occurs appears to be same for higher values of grain shear Reynolds number ($\frac{V_* d_{50}}{\nu} > 200$) and shifts with decrease in $\frac{V_* d_{50}}{\nu}$ for $\frac{V_* d_{50}}{\nu} < 200$. The magnitude of maximum value of K_B/d_{50} remains fairly constant in all the cases. With these as noticeable features, the model has been developed on similar lines for uniform sand grains randomly spaced case.

(i) Functional relationship between theoretical bed level and $\frac{d_{50} V_*}{\nu}$ and σ/d_{50}

Theoretical bed level ϵ , measured from the flat surface on which sand grains are stuck is function of geometry of the sand surface namely σ/d_{50} and state of flow represented in terms of $\frac{d_{50} V_*}{\nu}$. From the experimental observations it may be noted that at particular value of $\frac{d_{50} V_*}{\nu}$, the ϵ/d_{50} is maximum when σ/d_{50} is minimum, in the present investigation $\sigma/d_{50} = .05$ and decreases with increase in nonuniformity σ/d_{50} . This trend is observed in all cases. With an assumption that ϵ/d_{50} is purely

function of σ/d_{50} for higher values of $\frac{d_{50}V_*}{\gamma}$ and functions of both σ/d_{50} and $\frac{d_{50}V_*}{\gamma}$ for $\frac{d_{50}V_*}{\gamma} < 200$, an empirical equation is proposed as shown in Fig. 19

$$\frac{\varepsilon}{d_{50}} = \exp \left[- \left\{ 0.18 + \sqrt{\sigma/d_{50}} - (1 + \sigma/d_{50})^{1/3} \right. \right. \\ \left. \left. \exp 0.0144(47 - d_{50}^+) \right\} \right] = E_1 \quad (23)$$

Considering ε/d_{50} is function of σ/d_{50} and $\frac{d_{50}V_*}{\gamma}$ the plot of ε/d_{50} with $\sigma^+ + d_{50}^+$ was made as shown in the Fig. 20.

It may be seen that ε/d_{50} decreases monotonically with increase in $\sigma^+ + d_{50}^+$ and their functional relationship may be represented in the form of

$$\frac{\varepsilon}{d_{50}} = \frac{4.4}{1 + 0.026(\sigma^+ + d_{50}^+)} = E_2 \quad (24)$$

(ii) Functional relationship among Au^+ , ε^+ , d_{50}^+ and σ/d_{50}

Using the present experimental results, along with results of David, P.K. Mittal and S. Mittal, the plot of

$Au^+ - \frac{1}{x} \ln \varepsilon^+$ with $\sqrt{\sigma^+ \cdot d_{50}^+}$ is made in Fig. 21. The parameter $\sqrt{\sigma^+ \cdot d_{50}^+}$ was chosen with an idea that d_{50} represents average width of protrusions and σ represents the height of protrusions. The product of σd_{50} represents the

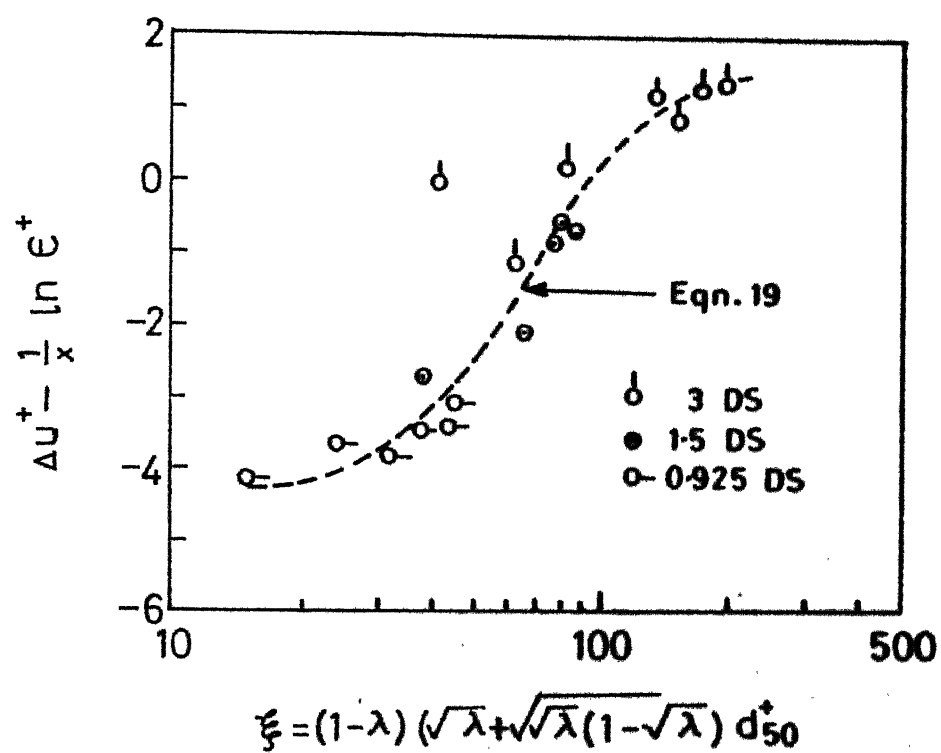


FIG 19 RELATIONSHIP BETWEEN $\Delta u^+, \epsilon^+, \lambda$ and d_{50}^+

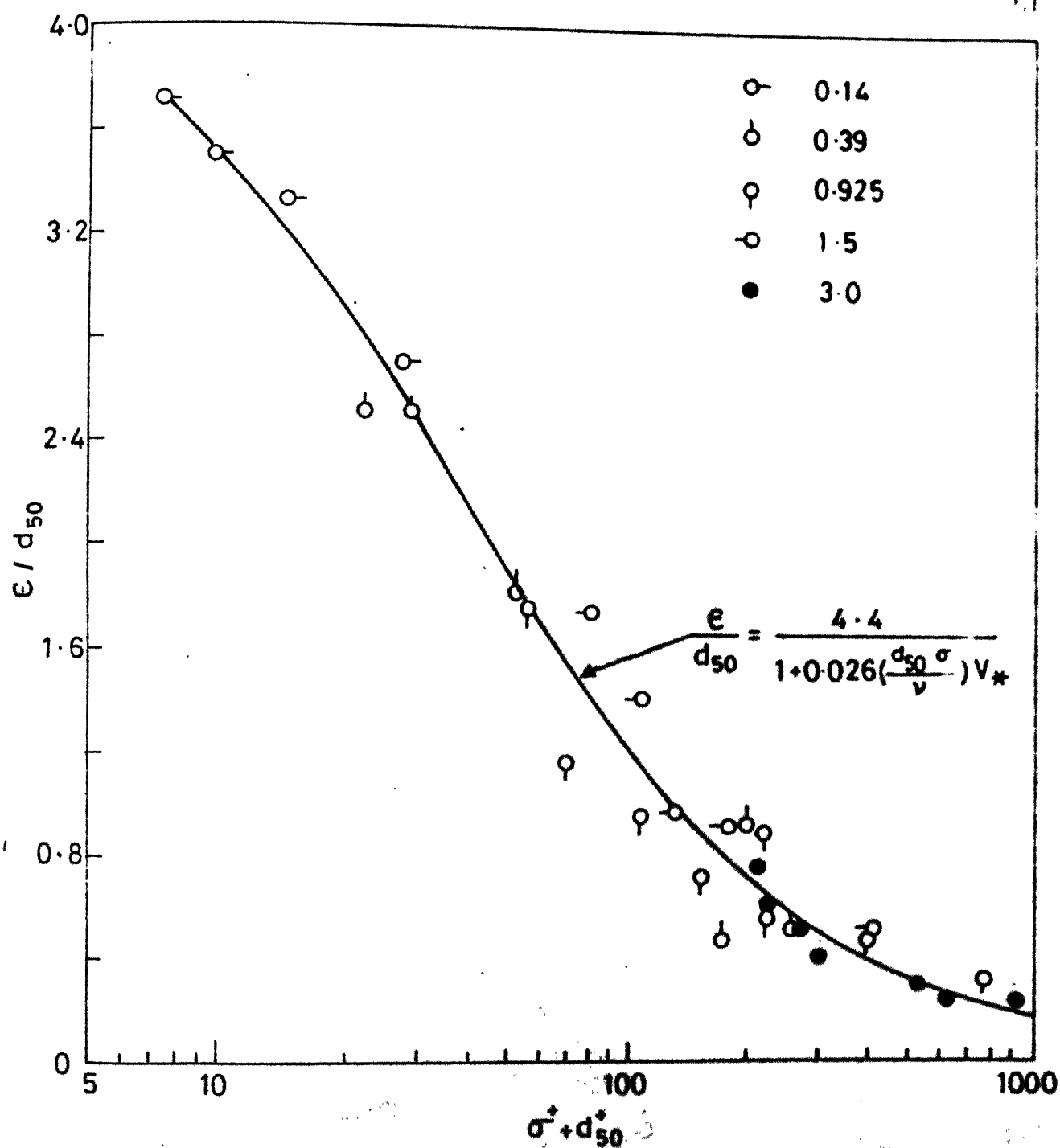
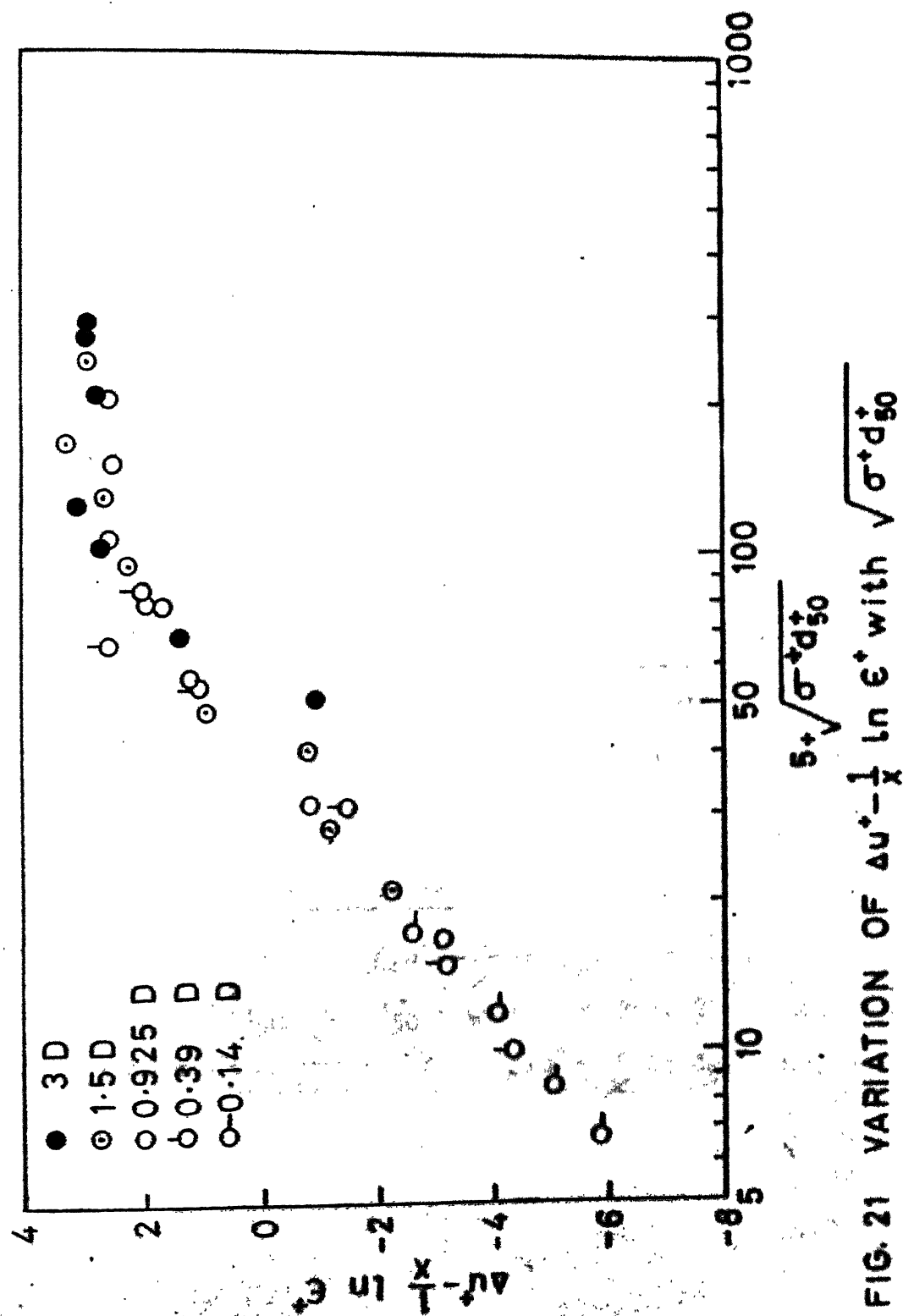


FIG.20 VARIATION OF ϵ/d_{50} with $\sigma^* + d_{50}$


 FIG. 21 VARIATION OF $\Delta u^* - \frac{1}{x} \ln \epsilon^*$ with $\sqrt{\sigma^* d_{50}^*}$

effective area of the protrusions facing the flow. The parameter $\sqrt{\sigma^+ d_{50}^+}$ represents with Grain Shear Reynolds number based on the square root of average effective area. The functional relationship between $\Delta u^+ - \frac{1}{\chi} \ln e^+$ and $\sqrt{\sigma^+ d_{50}^+}$ may be written as

$$\Delta u^+ - \frac{1}{\chi} \ln e^+ = \frac{1}{\chi} \left[\ln(2.718 + (.0028 d_{50}^+)^{3/2}) \right] \left[1 - \text{Exp. } 0.03 (35 - \sqrt{\sigma^+ d_{50}^+}) \right] = F_1 \quad (25)$$

Another functional relationship has been developed using $(\sigma^+ + d_{50}^+)$ as parameter. This functional form is represented as

$$\Delta u^+ - \frac{1}{\chi} \ln e^+ = 3 - 9.6 \text{ Exp. } - .016 \eta = F_2 \quad (26)$$

where $\eta = (\sigma^+ + d_{50}^+) (1 - \text{Exp. } (-\frac{88}{\sqrt{d_{50}^+}} \frac{\sigma}{d_{50}}))$

Both above equations are used in the development of model for roughness scales.

(iii) Model for roughness scale

Roughness scales $\Delta u^+ - \frac{1}{\chi} \ln d_{50}^+$ or $\frac{K_s}{d_{50}}$ are related with σ/d_{50} and d_{50}^+ using the Eqs. 23 or 24, 25 or 26. Using equation an expression for $\Delta u^+ - \frac{1}{\chi} \ln d_{50}^+$ may be written as

$$\Delta u^+ - \frac{1}{\chi} \ln d_{50}^+ = \frac{1}{\chi} \ln [E_1 \text{ or } E_2] + [F_1 \text{ or } F_2] \quad (27)$$

An expression for Nikuradse's roughness scale K_s/d_{50} may be written using Eqns. 9 and 27 as

$$\frac{K_s}{d_{50}} = - \frac{3.3}{d_{50}^+} + 3.215 [E_1 \text{ or } E_2] \text{Exp.} [\chi F_1 \text{ or } \chi F_2] \quad (28)$$

Among the combinations of E_1 or E_2 with F_1 or F_2 , from the computed values it was found that a combination of E_2 with F_1 gives a better representative values in comparison ^{with} experimental values. An expression for

$\Delta u^+ - \frac{1}{\chi} \ln d_{50}^+$ and K_s/d_{50} using this combination may be written as

$$\Delta u^+ - \frac{1}{\chi} \ln d_{50}^+ = \frac{1}{\chi} \ln \left[\frac{4.4}{1 + .026(\sigma^+ + d_{50}^+)} \right] + \frac{1}{\chi} \left[\ln(2.718 + (.0028 d_{50}^+)^{3/2}) \right] \times \left[1 - \text{Exp. } 0.03(35 - \sqrt{\sigma^+ + d_{50}^+}) \right] \quad (29)$$

and

$$\frac{K_s}{d_{50}} = - \frac{3.3}{d_{50}^+} + \frac{3.215 \times 4.4}{1 + .026(\sigma^+ + d_{50}^+)} \text{Exp} \left[\ln 2.718 + (.0028 d_{50}^+)^{3/2} \right] \times \left[1 - \text{Exp. } 0.03(35 - \sqrt{\sigma^+ + d_{50}^+}) \right] \quad (30)$$

Table 4 below shows the computed values of K_s/d_{50} with corresponding experimental values.

TABLE 4 : COMPUTED VALUES OF ROUGHNESS SCALES

$\frac{\sigma}{d_{50}}$	3D		$\frac{\sigma}{d_{50}}$	1.5D		$\frac{\sigma}{d_{50}}$	0.925 D	
	K_s/d_{50}			K_s/d_{50}			K_s/d_{50}	
	Exptt.	Computed		Exptt.	Computed		Exptt.	Computed
.051	1.75	3.25	.05	1.65	2.20	.047	1.55	1.93
.063	2.05	3.73	.11	2.45	3.20	.203	2.70	3.70
.08	3.45	4.30	.202	3.40	4.56	.642	3.90	5.65
.09	3.69	4.58	.35	4.20	5.60	1.302	4.60	6.03
.191	4.90	6.13	.65	4.65	6.25	2.37	5.00	5.33
.339	4.50	6.50	1.25	4.25	5.78	5.049	4.0	3.59
.781	3.40	5.53	1.75	3.70	5.13	12.00	2.60	1.80
1.317	2.90	4.41	4.80	2.05	2.74			
1.786	2.60	3.72	0.39D					
3.26	1.80	2.48	.052	1.30	1.87			
0.14D			.257	2.20	2.78			
.052	1.10	1.68	1.227	3.30	4.29			
.208	1.50	1.94	3.593	4.65	4.69			
.766	2.00	2.34	5.629	4.15	4.36			
2.120	3.05	2.67	9.567	3.35	3.63			

From table it may be observed that position of peak values coincide with position of peak occurrence of the experimental results. The trend in the variation follows the experimental values. However, the magnitudes of peak values are higher in comparison to corresponding experimental values. Also the magnitude of peak values increases with decrease in $\frac{d_{50}^V}{d_{50}^+}$, reaches a highest magnitude around $\frac{d_{50}^V}{d_{50}^+} \approx 100$ and decreases with further decrease in $\frac{d_{50}^V}{d_{50}^+}$ values.

E. General Comments

Development of models based on geometric parameters like \overline{Oh} , S_a or H_g are found to be inadequate to represent the roughness scales. Along with these geometric parameter, the median size also has to be considered. Further, consideration of the effect of state of flow has to be made.

From the models developed for uniform sand grain randomly spaced, and nonuniform sand grains densely packed, the trend in variations coincide with experimental values very nicely. The order of magnitude of roughness scales are also within + 20 per cent of the experimental values. However, a further look into these relations may help to achieve a close agreeable models.

An effort was made to develop a single model for uniform randomly spaced and nonuniform grains densely packed

based on the statistical parameters of surface protrusions namely, mean of protrusion heights and standard deviation of protrusion heights. This was not very successful and hence not reported.

CHAPTER IV

CONCLUSIONS AND RECOMMENDATIONS

A. General

Roughness of sand beds was investigated by measuring velocity distribution on flat sand beds in wind tunnel. Sand beds used are of two types namely, uniform sand grain size of 1.5 mm randomly spaced with 5 different roughness concentrations and beds having densely packed nonuniform sand grains with median value of 1.5 mm for 8 different nonuniformity values. Experiments were specially aimed to investigate the transitional state of flow. Flow parameters like shift in theoretical bed level z , shift in velocity scale Δu and bed shear velocity of the flow, V_* were computed from mean velocity data in the wall region using statistical method. The velocity distributions were analysed using these parameters and showed how roughness concentrations and nonuniformity parameters affect the velocity distributions. Velocity profiles are found to be represented by scales representing the roughness; in terms of Nikuradse's equivalent sand grain roughness K_s/d_{50} and shift in velocity scale $\Delta u^+ = \frac{1}{\kappa} \ln d_{50}^+$ and shift in length scale z/d_{50} . These scales are functionally to σ/d_{50} or λ and $\frac{d_{50} V_*}{\nu}$, using the present experimental data along with the data of

David, P.K. Mittal and S. Mittal. The following are the major conclusions based on the analysis of the experimental data.

B. Conclusions

1. The existence of transition in velocity scale Δu^+ in the region $70 < \frac{d_{50} V_*}{\gamma} < 200$ with different σ/d_{50} is established, experimentally.
2. The velocity scales and length scales represented as $\Delta u^+ = \frac{1}{\chi} \ln \epsilon^+$ and ϵ/d_{50} are found to be functionally related with λ or σ/d_{50} and $\frac{d_{50} V_*}{\gamma}$.
3. The models for predicting the roughness of sand beds in terms of shift in velocity scale $\Delta u^+ = \frac{1}{\chi} \ln d_{50}^+$ and Nikuradse's equivalent sand grain roughness K_s/d_{50} are developed. These models predict the experimental results fairly well.

C. Recommendations

Models developed for roughness scales are suitable for two separate cases namely uniform sand grains randomly spaced and nonuniform grains densely packed. A general method to be used for the both cases is needed to be developed.

Based on the some analysis carried out, it may be suggested that models should be based on the **statistical** parameters representing the surface of the beds. These statistical parameters may be of mean of heights and standard deviations of heights of protrusions of roughness elements.

CHAPTER V

BIBLIOGRAPHY

- (1933) Nikuradse, J., 'Stromungsgesetze in rauhen Rohren', Forschungsheft 361, V.D.I.
- (1936) Schlichting, H., 'Experimentelle Untersuchungen zum Rauheitsproblem', Ingenieur-Archive, Vol.VII, No.1, February.
- (1937) Colebrook, C.F. and White, C.M., 'Experiments with fluid friction in roughened pipes', Proceedings, Royal Soc. of London, Series A, Vol.161.
- (1949) Einstein, H.A. and El-Samni, E.S., 'Hydrodynamic force on a rough wall', Rev. Modern Phys., Vol.21, No.3.
- (1951) Moore, W.F., 'An Experimental Investigation of the Boundary Layer Development along a Rough Surface', Ph.D. Dissertation, State University of Iowa.
- (1952) Einstein, H.A. and Barbarossa, 'River Channel Roughness', Trans. ASCE, Vol. 117.
- (1954) Clauser, F.H., 'Turbulent boundary layers in adverse pressure gradients', Jl. of Aero. Sci., Vol.21.
- Hama, F.R., 'Boundary Layer Characteristics for Smooth and Rough Surfaces', Trans. SNAME, Vol.62.
- (1956) Clauser, F.H., 'Advances in Appld. Mechanics, 4.1.
- (1960) Albertson, M.L., Barton, J.R. and Simons, D.B., 'Fluid Mechanics for Engineers', Prentice-Hall, Inc., Englewood, Cliffs, N.J.

- (1962) Perry, A.E. and Joubert, P.N., 'Rough wall boundary layers in adverse pressure gradients', Jl. of Fluid Mechanics, Vol.17.
- (1964) O'Loughlin, E.M. and MacDonald, B.G., 'Some roughness-concentration effects on boundary resistance, La Houille Blanche, No.7.
- (1965) Batterman, D., 'Contribution a l'etude de la couche limite turbulente le long de plaques regueuses', Rapport 65-6, Centre Nat. de la Rech. Sci., Paris, France.
- (1966) Simons, D.B. and Richardson, E.V., 'Resistance to Flow in Alluvial Channels', U.S. Geological Survey, Professional Paper, 422-J.
- (1969) Perry, A.E., Schofield, W.H. and Joubert, P.N., 'Rough Wall Turbulent Boundary Layers', Jl. of Fluid Mechanics, Vol.37.
- (1971) Blinco, P.H. and Partheniades, E., Jl. of Hydr. Res. 9, 43.
- (1974) Kamphuis, 'Determination of Sand Roughness for Fixed Beds', Jl. of Hyd. Res., Vol.12, No.2.
White, C.M., 'Viscous Fluid Flow', McGraw-Hill Book Co., Inc., NY.
- (1977) Aswatha Narayana, P.A. 'Experimental Investigation of Turbulent Boundary Layer Over Smooth and Rough Surfaces', Delft University of Technology, Delft, The Netherlands.

- (1977) Mittal, P.K., 'Roughness of Nonuniform Sand Beds' ,
M.Tech. Dissertation, IIT Kanpur.
- Simons, D.B. and Senturk , F., 'Sediment Transport
Technology', Water Resources Publications, Fort
Collins, Colorado, U.S.A.
- (1978) Mittal, S., 'Roughness of Sand Beds having nonuniform
grain size distribution', M.Tech. Dissertation, IIT Kanpur.
- (1980) David, K.J., 'The Effect of Nonuniformity in Grain
Size on the Roughness of Sand Beds', A Thesis submitted
in partial fulfilment of the requirements for the
Ph.D. to the Department Civil Engg., IIT Kanpur.
- Sarin, A. 'Roughness of Sand Beds: Effect of Shape
and Arrangement Pattern', M.Tech. Dissertation, IIT/K.
- (1981) Aslam Mohd., 'Initiation of Motion: Effect of
Roughness Concentration, M.Tech. Dissertation, IIT/K.
- (1956) Cartwright and Longuet-Higgins, 'The Statistical
Distribution of Maximum of a Random Function',
Proceedings of Roy. Soc. London, A-237, pp.212-232.

CHAPTER VI

APPENDIX

Bed Series	Δ	$\frac{H_s}{d_{50}}$	$\frac{K_s}{H_s}$	S_o	$S_2 \times 10^3$	$S_4 \times 10^8$	η
	1	2	3	4	5	6	7
3.0 DS	0.01	0.56	0.50	0.30	2.05	0.25	0.67
	0.02	0.77	0.71	0.40	1.41	0.09	0.67
	0.065	1.08	1.57	0.96	4.49	0.04	0.69
	0.15	1.29	1.88	1.07	2.24	0.10	0.71
	0.202	1.57	1.88	1.58	2.70	0.12	0.79
	0.394	1.62	1.67	1.74	2.81	0.13	0.80
	0.608	1.56	1.47	2.02	0.86	0.02	0.90
1.50 DS	0.050	1.20	0.88	0.25	3.32	24.11	0.99
	0.150	1.05	1.90	0.21	0.73	0.05	0.72
	0.260	1.23	1.85	0.25	0.35	0.01	0.73
	0.400	1.57	1.46	0.38	0.46	0.01	0.79
	0.700	1.66	1.04	0.31	0.09	0.001	0.86
0.925 DS	0.100	0.85	1.29	10.10	83.70	12.35	0.65
	0.200	1.01	1.83	18.16	148.01	20.99	0.64
	0.300	1.12	1.83	8.67	22.77	1.06	0.66
	0.390	1.14	1.58	15.29	37.62	1.54	0.63
	0.470	1.14	1.48	8.54	7.41	0.10	0.60
	0.750	1.23	1.02	12.17	10.99	0.17	0.64

Contd.....

σ/a_{50}							
Bed Series	1	2	3	4	5	6 $\times 10^5$	7
3.00 D	0.051	1.40	1.53	1.21	0.08	0.51	0.95
	0.080	1.03	1.99	4.54	1.05	6.34	0.79
	0.090	1.04	3.31	4.54	1.17	7.44	0.77
	0.191	1.26	2.86	4.59	1.03	6.10	0.71
	0.339	1.37	1.92	4.71	1.07	6.21	0.78
	0.781	1.37	2.48	4.67	1.04	6.21	0.79
	1.317	1.73	1.68	4.90	1.05	6.04	0.79
	1.786	2.96	0.87	5.44	1.07	6.13	0.81
	3.260	5.43	0.33	12.68	1.24	6.65	0.90
1.5 D	0.050	1.26	1.31	0.50	0.012	0.075	0.98
	0.110	1.13	2.17	3.46	1.160	7.910	0.71
	0.202	1.17	2.91	3.49	1.150	7.69	0.715
	0.350	4.27	0.98	5.01	1.58	10.50	0.725
	0.650	4.83	0.96	5.36	1.65	10.60	0.723
	1.250	6.90	0.61	6.14	1.83	12.35	0.750
	1.750	8.50	0.50	13.60	1.95	11.90	0.790
	4.800	16.95	0.12	21.48	2.32	12.82	0.890
0.925 D	0.047	6.47	2.40	14.83	0.57	0.26	0.385
	0.203	1.55	1.70	13.26	1.86	11.90	0.920
	0.642	2.09	1.80	17.45	1.77	9.74	0.904
	1.302	1.71	2.70	15.11	1.67	9.33	0.900
	2.370	4.06	1.23	33.16	2.55	11.92	0.914
	5.049	4.25	1.00	21.96	2.33	9.72	0.864
	12.000	3.15	0.82	11.23	2.05	10.75	0.807

Contd.....

Bed Series	1	2	3	4	5	6	7
0.39 D	0.052	1.53	0.85	1.66	0.043	0.09	0.933
	0.257	1.89	1.16	3.00	0.090	0.055	0.974
	1.227	5.28	0.625	18.87	2.110	103.890	0.990
	3.593	5.51	0.84	16.61	2.682	14.960	0.843
	5.629	5.93	0.70	15.58	2.480	14.500	0.854
	9.567	4.13	0.80	5.71	1.200	6.760	0.790
0.14 D	0.052	1.712	0.64	0.46	0.010	0.039	0.970
	0.208	1.330	1.12	3.37	0.010	6.080	0.703
	0.766	3.205	0.624	3.917	1.170	7.230	0.718
	2.120	3.700	0.823	4.219	1.259	7.889	0.723

Bed Series	λ	\bar{h} (mm)	(mm^h)	\bar{a} (mm)	a (mm)	\bar{s} (mm)	s (mm)
	1	2	3	4	5	6	7
3.00 DS	0.01	0.139	0.631	2.86	0.43	45.27	28.87
	0.02	0.270	0.859	2.91	0.36	23.62	13.66
	0.065	0.562	1.171	2.96	0.23	11.70	8.55
	0.150	0.862	1.358	2.96	0.23	8.06	3.99
	0.262	1.294	1.486	2.97	0.21	6.41	2.74
	0.394	1.537	1.500	2.97	0.21	6.28	2.43
	0.608	2.250	1.299	2.94	0.28	8.52	3.43

Bed Series	1	2	3	4	5	6	7
1.5 DS	0.05	0.163	0.476	1.531	0.121	19.55	6.24
	0.15	0.245	0.566	1.521	0.146	17.33	7.12
	0.26	0.416	0.687	1.520	0.149	10.38	7.65
	0.40	0.687	0.770	1.530	0.124	7.42	4.05
	0.70	0.960	0.752	1.518	0.155	6.92	3.83
0.925 DS	0.10	0.120	0.326	0.986	0.082	17.06	11.54
	0.20	0.194	0.395	0.992	0.065	10.47	4.66
	0.30	0.234	0.424	0.987	0.080	8.84	4.44
	0.39	0.286	0.450	0.989	0.070	7.08	1.91
	0.47	0.314	0.464	0.984	0.088	6.26	1.32
	0.75	0.352	0.480	0.986	0.083	5.77	0.636

Bed Series	σ/a_{50}	2	3	4	5	6	7
1.5 D	0.05	1.66	0.505	0.794	0.554	7.18	3.70
	0.11	1.68	0.618	1.044	0.417	6.71	2.56
	0.20	1.75	0.630	0.992	0.715	6.89	2.88
	0.35	2.12	2.310	1.940	3.195	5.73	2.28
	0.65	2.35	2.590	4.172	8.950	7.75	3.23
	1.25	2.93	3.570	4.585	4.929	7.53	3.60
	1.75	3.25	4.250	6.750	6.870	7.03	3.12
	4.80	8.50	7.324	9.562	8.170	6.67	2.78